ORGANOMETALLICS

Article

pubs.acs.org/Organometallics

Methoxy-Functionalized *N*-Heterocyclic Carbenes

David J. Nelson, Alba Collado, Simone Manzini, Sebastien Meiries, Alexandra M. Z. Slawin, David B. Cordes, and Steven P. Nolan*

EaStCHEM School of Chemistry, University of St Andrews, North Haugh, St Andrews, Fife KY16 9ST, U.K.

Supporting Information

ABSTRACT: The effect of methoxy functionalization of three N-heterocyclic carbene ligands was assessed using a variety of methods. The steric environment of each carbene has been assessed in various coordination environments. The electronic properties, specifically the electron-donating character and π-accepting ability, have been evaluated using nickel and iridium complexes and selenium adducts, respectively. Comparisons with the parent systems have been made with respect to both electronic and steric properties. The carbenes **IPr^{OMe}**, **SIPr^{OMe}**, and **IPr*^{OMe}** have been found to be more electron donating than the parent systems **IPr**, **SIPr**, and **IPr*** and only slightly less π accepting, yet they exhibit similar steric properties.

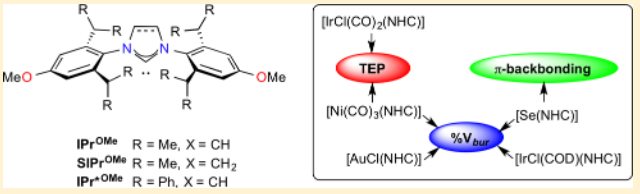

INTRODUCTION

N-heterocyclic carbenes (NHCs) are incredibly versatile ligands in organometallic chemistry[1,2] and have been employed with great success in a variety of applications such as ruthenium-catalyzed alkene metathesis[3,4] and palladium-catalyzed cross coupling.[5] Research within our group is focused on the synthesis and study of these interesting species, with particular focus on their application in the field of homogeneous catalysis. Metrics such as the percent buried volume (%V_{bur})[6] allow the steric bulk of NHCs to be quantified, while the Tolman electronic parameter (TEP)[7] allows for the comparison and quantification of their electronic properties,[8] with the aim of understanding how structure affects the properties of these ligands and the complexes to which they are coordinated. However, a detailed and quantitative comparison of these characteristics is not always straightforward.[9,10] Various model systems have been used to probe and quantify the numerous facets of the electronic properties of NHCs,[8,11−15] while the use of steric maps, calculated using the SambVca web application,[16] has allowed more detailed analysis of how NHCs can influence the steric environment around metal centers. Such evaluation and quantification are important, as they allow the appraisal of properties of new NHCs in the context of the vast body of literature that exists on the subject.

The variety and flexibility of synthetic routes to (4,5-dihydro)imidazolium-type NHC precursors has enabled a vast number of such ligands to be prepared,[17] with different functional groups in various positions. Plenio and co-workers have shown that modulation of the para substituent of *N*,*N*′-diarylimidazolylidenes can change the electronic character of the ligands, as determined by measurement of the TEP and by electrochemical experiments.[18] In other studies by the same group, π-face donation from the *N*-aryl substituents to the benzylidene ligand in second-generation ruthenium benzylidene complexes was revealed.[19,20] The presence of two distinct redox processes with different half-wave potentials for complexes bearing unsymmetrical NHC ligands was interpreted as evidence that the electronic communication from the *N*-aryl substituents to elsewhere on the complex did not occur exclusively via inductive and/or mesomeric effects over seven bonds to the metal center. In each case, **IMes** and **SIMes** (and variants thereof with different *para* substituents) were considered. More recently, Cavallo and co-workers have investigated this issue and presented computational evidence for an interaction between the ipso carbon of the *N*-aryl substituent and empty metal d orbitals in NHC-bearing transition-metal complexes.[21]

Munz et al. have shown that substitution of the para position of an NHC *N*-aryl substituent in chelated bis(NHC) palladium(II) complexes leads to greater changes in properties than functionalization at the *ortho* or *meta* positions.[22] We have found recently that *p*-methoxy functionalization of the aryl rings of the **IPr***, **IPent**, **IHept**, and **INon** ligands[23,24] (leading to the new ligands **IPent^{OMe}**, **IHept^{OMe}**, **INon^{OMe}**, and **IPr*^{OMe}**) improved the performance of palladium catalysts in C−N, C−C, and C−S bond formation reactions.[25−28] We wished to explore whether similar functionalization of **IPr** and **SIPr** might lead to ligands with valuable new properties (Chart 1). Therefore, a number of model systems bearing **IPr**, **SIPr**, **IPr***, **IPr^{OMe}**, **SIPr^{OMe}**, and **IPr*^{OMe}** have been studied, to fully explore the effect of the *p*-methoxy substituent. In particular, the effect of this structural modification on the value of a number of common metrics was explored, to see if these could be correlated with the improved catalytic activity of metal complexes bearing these ligands and indeed whether these metrics could quantify the differences in their properties.

Received: February 22, 2014
Published: April 10, 2014

   dx.doi.org/10.1021/om5001919 | *Organometallics* 2014, 33, 2048−2058

Chart 1. Some Common NHC ligands and Their Methoxy Analogues

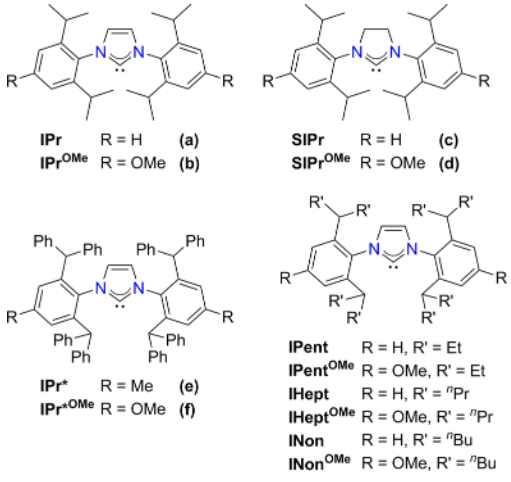

RESULTS AND DISCUSSION

Synthesis of Free Carbenes. The syntheses of **IPr**, **SIPr**, **IPr***, and **IPr*^{OMe}** have been described previously.[25,29−31] The syntheses of the salts **IPr^{OMe}**·HCl and **SIPr^{OMe}**·HCl have also been disclosed;[32] the key step in their synthesis is a copper-catalyzed Ullman coupling to generate the requisite 2,6-di*iso*propyl-4-methoxyaniline, which is followed by straightforward and established steps to yield the carbene salts. The free carbenes **IPr^{OMe}** and **SIPr^{OMe}** were prepared by deprotonation of the corresponding HBF_4 salts (prepared by salt metathesis) using NaH plus catalytic KO^{t}Bu, in an argon-filled glovebox

Scheme 1

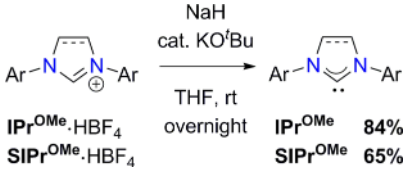

(Scheme 1). These carbenes were characterized by ^{1}H and ^{13}C{^{1}H} NMR spectroscopy. The key δ_C(carbene) chemical shifts for **IPr^{OMe}**, **SIPr^{OMe}**, and **IPr*^{OMe}** were found to be at 221.6 (C_6D_6), 245.0 (C_6D_6), and 221.8 (THF-d_8) ppm (compared to 220.6 (C_6D_6), 244.0 (C_6D_6), and 220.0 (THF-d_8) ppm for **IPr**, **SIPr**, and **IPr***).[14,25,31] The methoxy functionality shifts the carbene signals slightly downfield, suggesting that the electronic effects of methoxy substitution are not negligible even in the free carbene.

Synthesis of Model Complexes. Four classes of model compounds (**1**−**5**) bearing these NHCs (NHC: **a**, IPr; **b**, IPr^{OMe}; **c**, SIPr; **d**, SIPr^{OMe}; **e**, IPr*; **f**, IPr*^{OMe}) were prepared, to allow the characterization of their electronic and steric properties.

Linear Au(I) complexes of the form [AuCl(NHC)] are excellent models with which to evaluate the steric properties of new ligands;[6] the linear geometry enables NHC ligands to adopt their preferred conformation without interacting with other ligands present on the metal center. Notably, these can be prepared directly from the imidazolium salt, without the need to employ the free carbene.[33] The syntheses and crystal structures of the parent species bearing **IPr** (**1a**),[34] **SIPr** (**1c**),[35] and (**IPr***) (**1e**)[31] have been reported previously. The new complexes [AuCl(**IPr^{OMe}**)] (**1b**), [AuCl(**SIPr^{OMe}**)] (**1d**), and [AuCl(**IPr*^{OMe}**)] (**1f**) were prepared using the recently disclosed general methodology (Scheme 2).[33] Heating the

Scheme 2

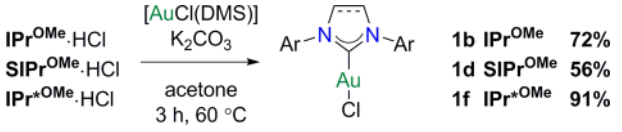

NHC precursor salt (**IPr^{OMe}**·HCl, **SIPr^{OMe}**·HCl, or **IPr*^{OMe}**·HCl) with [AuCl(DMS)][36] in acetone in the presence of a mild base (K_2CO_3) allowed the preparation of the corresponding analytically pure [AuCl(NHC)] complexes **1b**,**d**,**f** as white solids in 72%, 56% and 91% yields, respectively. Complex **1d** is poorly soluble in acetone and dichloromethane, in contrast to the vast majority of [AuCl(NHC)] complexes, which may be the cause of the poorer yield of this species. Catalytic applications of these complexes and their derivatives will be reported in due course.

Single crystals of the new complexes were grown for X-ray analysis by slowly diffusing pentane into a dichloromethane (for **1b**,**d**) or benzene (**1f**) solution (Figure 1). All three present the expected linear geometry about the gold(I) center.

Nickel carbonyl complexes of the form [Ni(CO)$_3$(NHC)] have been used to extend the evaluation of the Tolman electronic parameter,[7] traditionally used to compare the electronic properties of phosphine ligands, to the study of NHC ligands.[8] Infrared spectroscopic analysis of these complexes indicates the electron density of the metal center by probing its ability to engage in d to π^* back-bonding, which weakens the carbon−oxygen bond. It is therefore a measure of a combination of the σ-donating and π-accepting properties of the NHC. In addition, these complexes provide excellent examples of tetrahedral NHC-bearing complexes, allowing further evaluation of the steric behavior of the NHC ligand via their crystal structures. The syntheses and characterization of [Ni(CO)$_3$(**IPr**)] (**2a**), [Ni(CO)$_3$(**SIPr**)] (**2c**),[8] [Ni(CO)$_3$(**IPr***)] (**2e**),[37] and [Ni(CO)$_3$(**IPr*^{OMe}**)] (**2f**)[25] have been reported previously. New complexes were prepared via the addition of [Ni(CO)$_4$] to a THF solution of the free carbene, yielding the complexes [Ni(CO)$_3$(**IPr^{OMe}**)] (**2b**) and [Ni(CO)$_3$(**SIPr^{OMe}**)] (**2d**) in 57% and 93% yields, respectively (Scheme 3). Crystals suitable for X-ray diffraction analysis were prepared by slow diffusion of pentane into a saturated solution of each complex in benzene (Figure 2).

While the TEP has classically been determined via the use of [Ni(CO)$_3$L] complexes (where L is a phosphine or NHC), the use of [IrCl(CO)$_2$L] or [RhCl(CO)$_2$L] complexes is more convenient, is more accessible, and avoids the use of highly hazardous [Ni(CO)$_4$].[11,12,38] Recent work has allowed the development of useful correlations to translate the stretching frequencies of the carbonyl ligands in these complexes into values that can be compared to those determined using the nickel system.[9,10] Here, the use of the iridium system was explored for two reasons: (i) to provide additional data on the electronic character of the metal centers in complexes bearing these new NHCs, *via* IR spectroscopy, and (ii) to evaluate the steric bulk of the ligands in a third coordination environment, namely square planar, which is relevant to palladium(II)

dx.doi.org/10.1021/om5001919 | *Organometallics* 2014, 33, 2048−2058

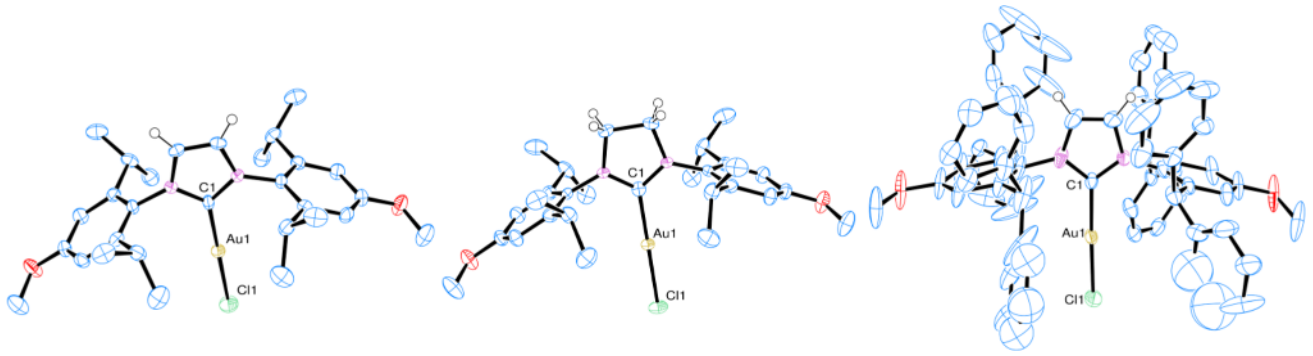

Figure 1. X-ray crystal structures of (left) [AuCl(**IPr**^{OMe})] (**1b**), (center) [AuCl(**SIPr**^{OMe})] (**1d**), and (right) [AuCl(**IPr***^{OMe})] (**1f**). Thermal ellipsoids are drawn at the 50% probability level, and most H atoms are excluded for clarity.

Scheme 3

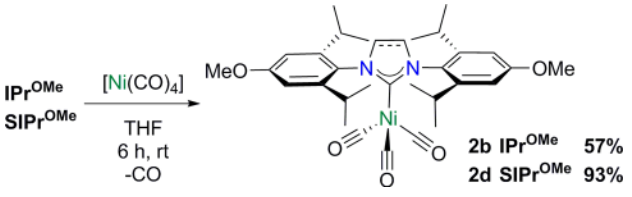

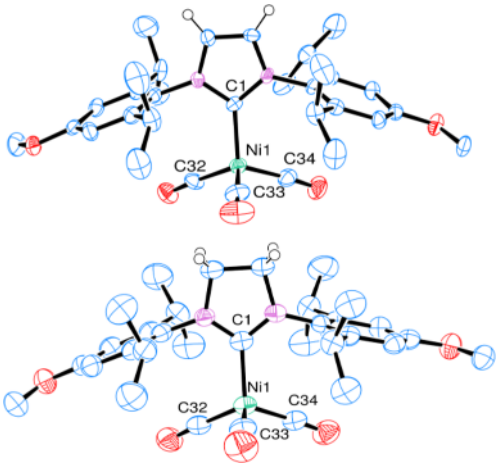

Figure 2. X-ray crystal structures of (top) [Ni(CO)$_3$(**IPr**^{OMe})] (**2b**) and (bottom) [Ni(CO)$_3$(**SIPr**^{OMe})] (**2d**). Thermal ellipsoids are drawn at the 50% probability level, and most H atoms are excluded for clarity.

Scheme 4

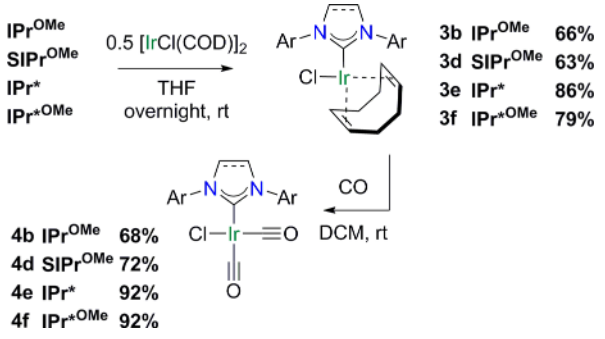

complexes,[39] also of d^8 configuration, that are important precatalysts and catalytic intermediates. [IrCl(CO)$_2$(**IPr**)] (**4a**) and [IrCl(CO)$_2$(**SIPr**)] (**4c**) have been reported previously.[11] New [IrCl(COD)(NHC)] complexes were prepared first, by addition of the carbene to a THF solution of [IrCl(COD)]$_2$. [IrCl(COD)(**IPr**^{OMe})] (**3b**), [IrCl(COD)(**SIPr**^{OMe})] (**3d**), [IrCl(COD)(**IPr***)] (**3e**), and [IrCl(COD)(**IPr***^{OMe})] (**3f**) were isolated in 63−86% yields as analytically pure yellow microcrystalline solids (Scheme 4). Single crystals of **3b**,**d**−**f** suitable for X-ray diffraction studies were grown (Figure 3).

Exposing these species, in DCM solution, to carbon monoxide yielded the desired *cis*-dicarbonyl complexes **4b**,**4d**−**f**. The cis arrangement of the carbonyl ligands was confirmed by IR and $^{13}C\{^1H\}$ NMR spectroscopy. While complexes of this type are typically air and moisture stable, all attempts to prepare and purify **4b** on the bench unexpectedly led to decomposition. The synthesis and purification of **4b** was therefore carried out under rigorously air- and moisture-free conditions using glovebox and Schlenk techniques.

While the TEP quantifies the overall ability of the metal center to engage in d to π^* back-bonding, it does not separate the contributions from σ and π bonding between the NHC and the metal center; it requires the assumption that all ligands being compared are similar in terms of π-accepting ability. The latter can contribute significantly to the overall bonding between the NHC and the metal center.[9,40] Three methods have been proposed to assess the contribution of d−π interactions to the NHC−metal bond. Analysis of δ_{Pt} (via the ^{195}Pt nuclide) and $^1J_{Pt-C}$ for [PtCl$_2$(DMSO)(NHC)] complexes allows the electron density at the metal and d to π back-bonding contributions to be investigated separately.[13] However, this requires detection of ^{195}Pt satellites for a signal that is typically very weak in the $^{13}C\{^1H\}$ NMR spectrum, thus necessitating long NMR experiment times and large quantities of expensive platinum. Bertrand and co-workers recently proposed the use of phosphinidene adducts [PPh(NHC)], prepared in two synthetic steps, to probe π back-bonding via the δ_P chemical shift on the ^{31}P NMR spectrum.[14] Ganter and co-workers reported the use of selenoureas, prepared in one synthetic step by deprotonation of the imidazolium salt in the presence of excess selenium, to probe π back-bonding via the δ_{Se} chemical shift on the ^{77}Se NMR spectrum.[15] In both of the latter examples, adducts might be viewed as existing between two extremes: one where the NHC−E bond has single-bond character and one where it has double-bond character. In the former, there is little π back-bonding, while in the latter this occurs to a considerable extent (Figure 4). Further studies are underway within our group to explore this proposed relationship between chemical shift and electronic structure.

dx.doi.org/10.1021/om5001919 | *Organometallics* 2014, 33, 2048−2058

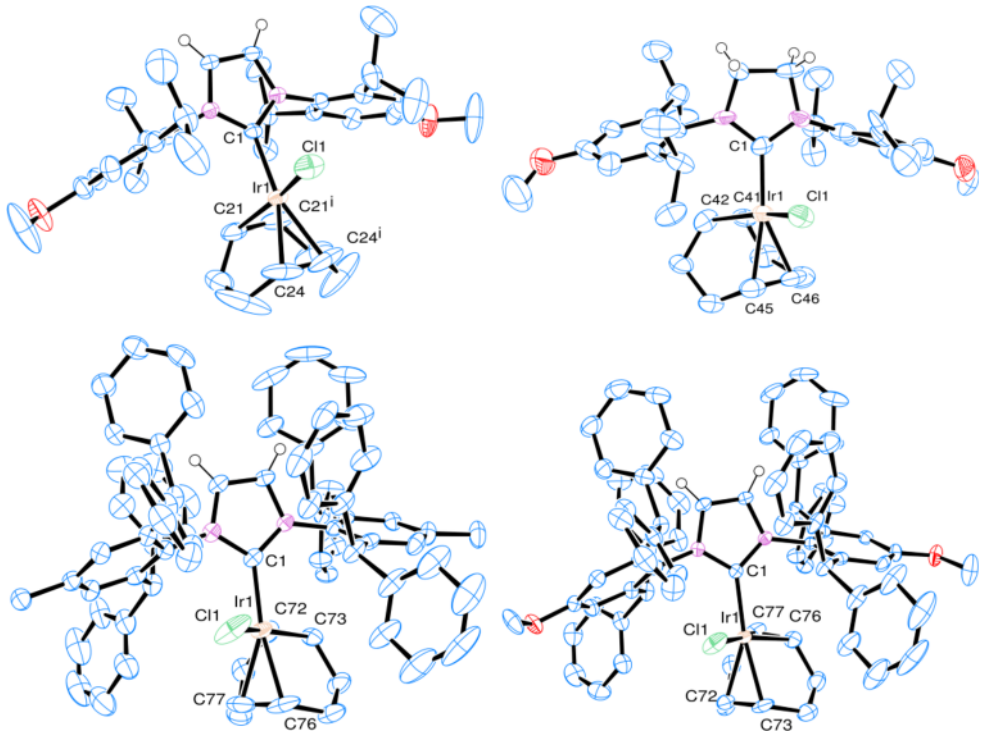

Figure 3. X-ray crystal structures of (top left) [IrCl(COD)(**IPr**^{OMe})] (**3b**), (top right) [IrCl(COD)(**SIPr**^{OMe})] (**3d**), (bottom left) [IrCl(COD)(**IPr***)] (**3e**), and (bottom right) [IrCl(COD)(**IPr***^{OMe})] (**3f**). Thermal ellipsoids are drawn at the 50% probability level, and most H atoms are excluded for clarity.

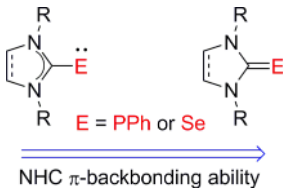

Figure 4. Phosphinidene and selenium adducts as probes of π backbonding to NHCs.

The use of selenium adducts was selected, due to the simpler synthetic protocol and the stability of the products. A THF solution of each free carbene was prepared in the glovebox and added via cannula to a Schlenk flask containing excess selenium (Scheme 5). The desired adducts were obtained in 66−96%

Scheme 5

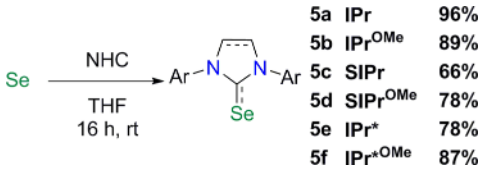

5a	**IPr**	**96%**
5b	**IPr**^{OMe}	**89%**
5c	**SIPr**	**66%**
5d	**SIPr**^{OMe}	**78%**
5e	**IPr***	**78%**
5f	**IPr***^{OMe}	**87%**

yields, as analytically pure white or light tan solids, after workup in air using undried/nondegassed solvents. Crystal structures were obtained for all six adducts, via crystallization by slow diffusion of pentane into a solution of the selenourea in chloroform, DCM, or acetone (Figure 5).

Full characterization data for complexes **1**−**5** can be found in the Experimental Section. With these data in hand, the steric and electronic properties of the ligands were systematically evaluated and compared to those of the corresponding parent carbenes.

Steric Properties. The steric properties were first evaluated by calculating the percent buried volume (%V_{bur})[6] for each of the gold, nickel, and iridium complexes (**1**−**3**), using the SambVca web application (Table 1).[16] Crystal structures were obtained from the literature for [AuCl(**IPr**)] (**1a**),[34] [AuCl(**SIPr**)] (**1c**),[35] [AuCl(**IPr***)] (**1e**),[31] [Ni(CO)$_3$(**IPr**)] (**2a**), [Ni(CO)$_3$(**SIPr**)] (**2d**),[8] [Ni(CO)$_3$(**IPr***)] (**2e**),[37] [Ni(CO)$_3$(**IPr***^{OMe})] (**2f**),[25] [IrCl(COD)(**IPr**)] (**3a**), and [IrCl(COD)(**SIPr**)] (**3c**).[11] Buried volumes were recalculated for each of these structures, to ensure accuracy in the comparisons between ligands.

Comparison of the buried volume for each methoxycarbene with that of its parent congener typically revealed a very modest difference in steric impact. For the iridium system, there was effectively no difference in the steric impact, especially given that for **3a,c** there is a *ca.* 2% difference in buried volume between the two independent molecules in each case. For nickel, methoxylation led to a 2.5% decrease in the bulk of **IPr** yet a 1% increase in the bulk of **IPr***. In the case of the linear two-coordinate gold(I) complexes, where the greatest differences in steric bulk typically are manifested, the biggest difference was for **IPr*** to **IPr***^{OMe}, where the methoxy functionalization decreased the buried volume by 3.3%. The use of solid-state structural data to infer the solution-state properties is fraught with difficulties, as packing effects can effect considerable changes in buried volumes. Complexes **2a** and **3a,c** contain two independent molecules, between which buried volumes vary by 0.2−2.1%. If the value of 2% is adopted as an uncertainty in each buried volume, then only the differences between **2a**/**2b** and **1e**/**1f** can be considered to be

dx.doi.org/10.1021/om5001919 | *Organometallics* 2014, 33, 2048−2058

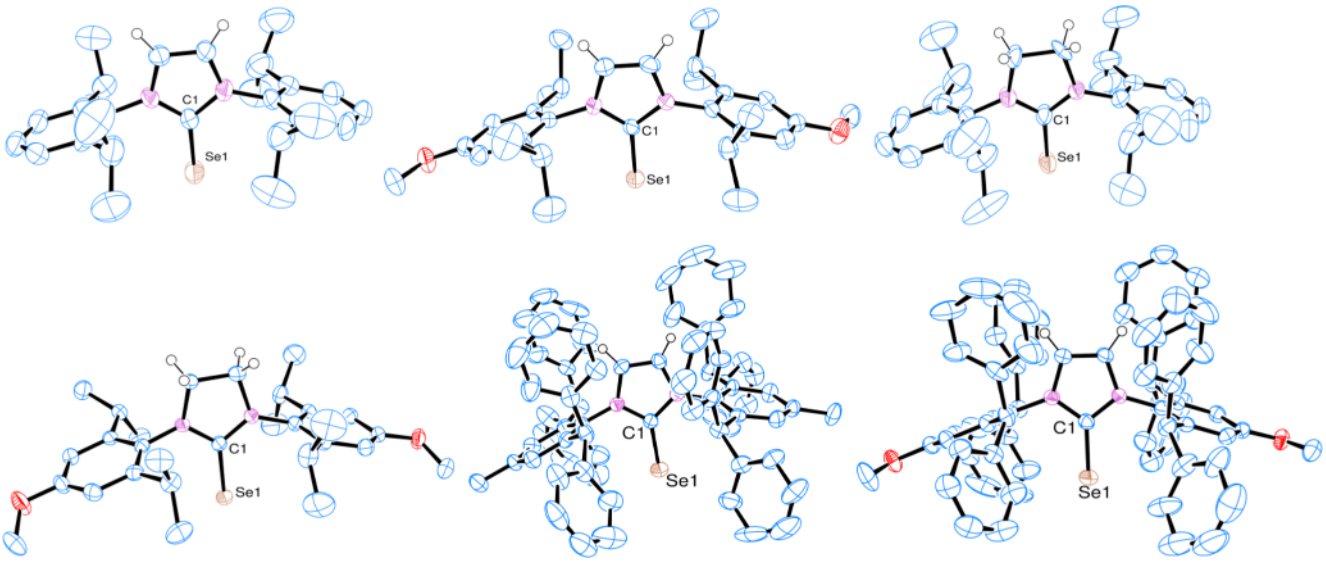

Figure 5. Crystal structures of selenoureas (top left) [Se(IPr)] (**5a**), (top middle) [Se(IPr^{OMe})] (**5b**), (top right) [Se(SIPr)] (**5c**), (bottom left) [Se(SIPr^{OMe})] (**5d**), (bottom middle) [Se(IPr*)] (**5e**), and (bottom right) [Se(IPr*^{OMe})] (**5f**). Thermal ellipsoids are drawn at the 50% probability level, while most H atoms are excluded.

Table 1. Percent Buried Volumes (%V_{bur}) for Complexes 1–3,[a] Assessed using the SambVca Web Application[16]

NHC	[Au] (**1**)	[Ni] (**2**)	[Ir] (**3**)
IPr (**a**)	44.5[b]	38.3, 38.1[c]	33.9, 36.0[d]
IPr^{OMe} (**b**)	45.6	35.8	33.3
SIPr (**c**)	47.0[e]	39.0[c]	36.4, 34.5[d]
SIPr^{OMe} (**d**)	46.5	39.1	36.1
IPr* (**e**)	50.4[f]	38.8[g]	37.9
IPr*^{OMe} (**f**)	47.1	39.8[h]	37.9

[a]Parameters: 3.5 Å sphere radius, 2.00 Å bond length, 0.10 Å mesh spacing, H atoms excluded. For multiple independent molecules, %V_{bur} is calculated for each. [b]Structure from ref 34. [c]Structure from ref 8. [d]Structure from ref 11. [e]Structure from ref 35. [f]Structure from ref 31. [g]Structure from ref 37. [h]Structure from ref 25.

significant, with methoxylation leading to a slight reduction in buried volume in each case.

The methoxy-NHCs adopt very similar conformations, as illustrated by overlaying the crystal structures of [AuCl(NHC)] complexes with the corresponding [AuCl(NHC^{OMe})] structures (Figure 6).

Steric maps were prepared to survey the steric environment around the metal center in more detail. Figure 7 shows those generated for [AuCl(NHC)] complexes **1a–f**, as this environment should reveal the largest differences in the steric profile of ligands (steric maps for **2a–f** and **3a–f** can be found in the Supporting Information). Again, only very small differences were obtained, suggesting that the methoxy functionality has very little influence on the conformation and steric bulk of the NHC ligand.

Notably, the [AuCl(NHC)] model is favored for the assessment of the steric impact of the NHC, due to the linear geometry of the AuCl fragment being in a position to avoid repulsive interactions with the NHC ligand. With crystal structure data for selenourea adducts in hand, the buried volumes of the ligands in these species were assessed using Samb*V*ca (Table 2). A fixed Se–C distance of 1.8 Å was used, to reflect the shorter Se–C bond in comparison to bonds between NHCs and transition-metal centers. If these

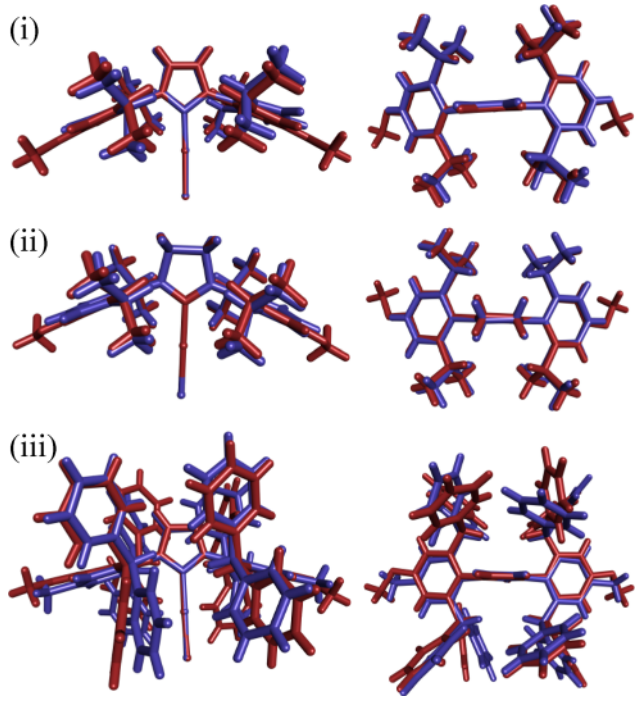

Figure 6. Overlays of the crystal structures of (i) [AuCl(**IPr**)] (**1a**) and [AuCl(**IPr^{OMe}**)] (**1b**), (ii) [AuCl(**SIPr**)] (**1c**) and [AuCl(**SIPr^{OMe}**)] (**1d**), and (iii) [AuCl(**IPr***)] (**1e**) and [AuCl(**IPr*^{OMe}**)] (**1f**).

selenoureas could provide a similar means of assessing steric impact, the synthesis of gold(I) complexes, which requires expensive starting materials, might be avoidable. Interestingly, the buried volumes for each of the NHCs are lower on selenium compounds **5** than on linear gold(I) species **1**, typically by 3–5%, even with a much shorter distance between the carbene and the sphere center (1.8 Å vs 2.0 Å). In addition, the same trend is not evident: when IPr, SIPr, and IPr* are compared to their methoxy-functionalized analogues, opposite trends in %V_{bur} are observed in comparison to the [AuCl-

dx.doi.org/10.1021/om5001919 | *Organometallics* 2014, 33, 2048–2058

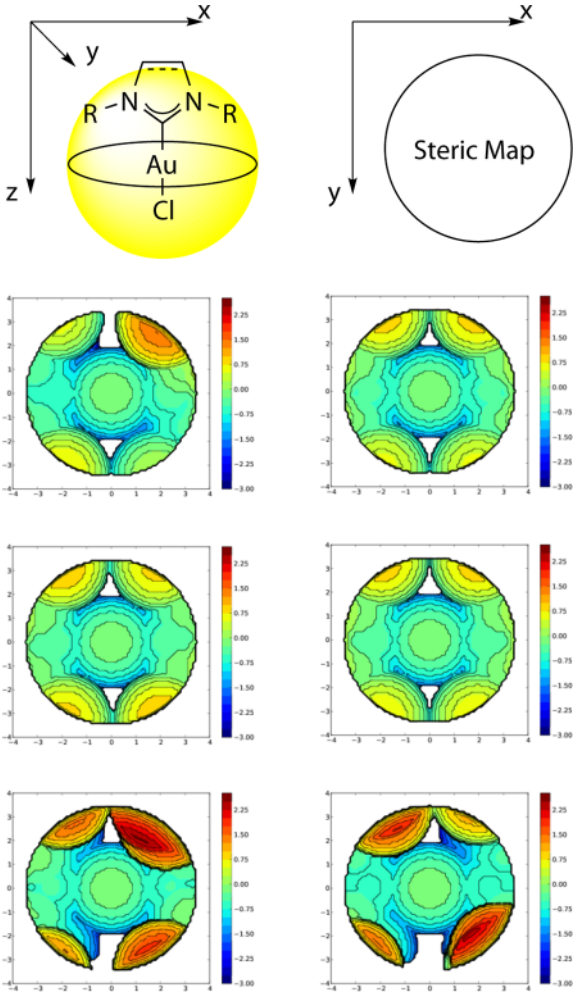

Figure 7. Steric maps of [AuCl(NHC)] complexes **1a–f** (NHC = **SIPr**, **IPr**, **IPr***, **SIPr^{OMe}**, **IPr^{OMe}**, **IPr*^{OMe}**), generated using the SambVca software (3.5 Å sphere, 0.10 Å mesh spacing, Bondi radii scaled by 1.17, H atoms omitted). Areas are shaded from blue to red according to the steric bulk protruding along the *z* axis: i.e., from the NHC ligand toward the gold center.

Table 2. Percent Buried Volumes (%V_{bur}) for Complexes 5a–f,[a] Assessed using the SambVca Web Application

NHC	[Se] (**5**)	NHC	[Se] (**5**)
IPr (**a**)	43.1	**IPr^{OMe}** (**b**)	41.0
SIPr (**c**)	44.6	**SIPr^{OMe}** (**d**)	47.2
IPr* (**e**)	47.8	**IPr*^{OMe}** (**f**)	48.6

[a]Parameters: 3.5 Å sphere radius, 1.80 Å bond length, 0.10 Å mesh spacing, H atoms excluded.

(NHC)] system (alternative C–Se bond lengths provide the same trend; see the Supporting Information). Notably, while selenium has a smaller covalent radius than gold (1.20 Å versus 1.36 Å),[41] it has a larger van der Waals radius (1.90 Å versus 1.66 Å),[42] which might explain the decreased %V_{bur}. Selenium adducts of this type are therefore not appropriate models to assess the steric impact of NHCs, and the [AuCl(NHC)] system remains the preferred option.

It can be seen from this assessment that functionalization of the para position of the *N*-aryl substituent can be achieved without inducing significant differences in the steric properties of the ligand (typically <2% difference in %V_{bur}). Such decoupling of properties can allow for careful tuning of specific characteristics.

Electronic Properties. The effect of methoxy substitution on the electron-donating ability of the carbenes was assessed using the TEP, which was calculated in two ways. The first method uses the IR spectroscopic analysis of [Ni(CO)$_3$(NHC)] (**2**), using the A_1 vibration as an indication of how much the carbonyl bond has been weakened by d to π^* back-donation.[7,8] The second method relies on the same principle but utilizes [IrCl(CO)$_2$(NHC)] complexes (**4**) instead, averaging ν_{CO}.[11] The TEP can be determined from the average of ν_{CO} by using eq 1.[11] Data obtained for **2** and **4** are recorded in Table 3.

$$\text{TEP} = (0.847 \times \nu_{CO}(\text{av})) + 336\ \text{cm}^{-1} \quad (1)$$

Table 3. Tolman Electronic Parameter Values for Methoxy-Functionalized Carbenes versus the Parent Analogues

NHC	TEP(Ni)[a]/cm^{-1}	av ν_{CO}(Ir)[b]/cm^{-1}	TEP(Ir)[c]/cm^{-1}
IPr (**a**)	2051.5[d]	2023.9[e]	2050.2
IPr^{OMe} (**b**)	2049.9	2023.4	2049.8
SIPr (**c**)	2052.2[d]	2024.9[e]	2051.0
SIPr^{OMe} (**d**)	2050.3	2024.4	2050.7
IPr* (**e**)	2052.7[f]	2025.6	2051.7
IPr*^{OMe} (**f**)	2051.1[g]	2025.3	2051.4

[a]In DCM solution. [b]Average of *cis*- and *trans*-CO vibrations, in DCM solution. [c]Using the linear regression in eq 1, from ref 11. [d]From ref 8. [e]From ref 11. [f]From ref 37. [g]From ref 25.

For the iridium complexes **4**, the differences in the average CO stretching frequencies between the methoxy series and the parent series are very small, typically only 0.3–0.5 cm^{-1}. The differences between the stretching frequencies of each carbonyl ligand (*cis* and *trans* to the NHC) are approximately the same. However, the observed differences for the nickel complexes are larger, at 1.6–1.9 cm^{-1}, suggesting that these two systems are not completely equivalent for the determination of TEP. Notably, the former system contains two carbonyl ligands directly *cis* and *trans* to the NHC, while the latter contains three carbonyl ligands that lie at a ca. 109° angle with respect to the NHC. The orbitals with which the NHC and carbonyl ligands interact in each complex are therefore different. In each case the NHC ligands bearing a *p*-methoxy substituent were found to render the metal center more electron-rich, in agreement with analogous studies of **IMes** and derivatives.[18] It should be noted that while the TEP is typically quoted to one decimal place, such accuracy, especially between different spectrometers, is unlikely to be attained, which is a key weakness of this approach.

Bearing in mind the aforementioned limitations of the TEP regarding σ donation versus π back-bonding, the latter was assessed separately. By understanding how the π back-bonding ability of the carbene changes with substitution pattern, the results from TEP measurements can be placed into context. For the present work, the single-step procedure utilizing selenium was most convenient.[15] The selenium adducts **5** of all six NHCs were prepared. Characterization by ^{1}H and ^{13}C{^{1}H} NMR spectroscopy was carried out in CDCl$_3$, while ^{77}Se{^{1}H} analysis was performed in acetone-d_6 to allow comparison with the literature values. However, due to poor solubility, ^{77}Se{^{1}H}

dx.doi.org/10.1021/om5001919 | *Organometallics* 2014, 33, 2048–2058

analyses of [Se(**IPr***)] (**5e**) and [Se(**IPr***^{OMe})] (**5f**) could not be carried out in acetone-d_6; it was not even possible to acquire publishable ^{1}H NMR spectra of **5e**,**f** in this solvent. While this precludes detailed comparisons with literature data recorded in acetone-d_6, it is still possible to compare **IPr*** and **IPr***^{OMe} on the basis of results obtained in $CDCl_3$. In addition, **5a**−**d** were analyzed in $CDCl_3$ in order to facilitate interpretation of the data. The results of the ^{77}Se{^{1}H} NMR spectroscopic analyses of the selenium adducts can be found in Table 4.

Table 4. Measurement of the π-Accepting Properties of NHCs using Selenium Adducts[a]

	δ_{Se}(parent)/ppm		δ_{Se}(methoxy)/ppm	
NHC	acetone-d_6	$CDCl_3$	acetone-d_6	$CDCl_3$
IPr	87 (87)[b]	90	83	87
SIPr	181 (181)[b]	190	177	185
IPr*	[c]	106	[c]	104

[a] ^{77}Se{^{1}H} NMR spectroscopy was carried out in acetone-d_6 at 300 K. [b] Values in parentheses from ref 15. [c] Insoluble in acetone-d_6.

It can be seen from these data that IPr*-based ligands are slightly more π-accepting than IPr-type ligands ($\Delta\delta_{Se}$ = ca. 15 ppm). Notably, the methoxy-substituted carbenes exhibit only a very slightly lower degree of π-accepting ability in comparison to the parent ligands ($\Delta\delta_{Se}$ = 2−4 ppm). Further, these results suggest that differences in TEP between *p*-methoxy-functionalized bis(aryl) NHCs and their parent congeners are most likely a result of changes to the σ-donating ability of the NHC, rather than including a contribution from π acceptance. However, a quantitative scale allowing the full deconvolution of σ and π bonding by experimental means has still not been developed.

CONCLUSIONS

In conclusion, we have synthesized and fully characterized the new NHC ligands **IPr**^{OMe} and **SIPr**^{OMe}. In addition, the related **IPr***^{OMe} ligand was characterized in further detail. At each point, state-of-the-art techniques have been used to interrogate the steric and electronic properties of these modified NHCs; this contribution represents a detailed study of the many aspects of the character of these NHCs.

The steric impact of the methoxy-NHCs was found to be almost identical with that of the parent ligands, except for two examples where the methoxy-NHCs exhibited slightly smaller buried volumes. Notably, these are derived from solid-state structures; thus, it is difficult to understand whether this is due to the effect the methoxy group has on the ligand conformation or to its effect on the packing in the crystal structure. In addition, only very small differences were observed in the electronic properties of these ligands, with <2 cm^{-1} differences in TEP. However, in each case, the methoxy-functionalized analogue was found to have a lower TEP, reflecting its more electron-donating nature. The use of selenourea adducts to explore π back-bonding suggest that methoxy functionalization does not have an effect on this property.

Overall, only very modest differences in properties have been discovered. The challenge remains to understand how this structural modification can exert such a considerable effect on the catalytic activity of palladium complexes.[25,28] Work in our laboratories to further apply these ligands in new complexes in organometallic chemistry and catalysis is currently underway.

EXPERIMENTAL SECTION

General Considerations. All manipulations were carried out in an Ar-filled glovebox using dry, degassed solvents unless otherwise stated. **IPr**, **SIPr**,[29,30] **IPr***^{OMe}·HCl and **IPr***^{OMe},[25] **IPr***,[31] and **IPr**^{OMe}·HCl and **SIPr**^{OMe}·HCl[32] were prepared according to the reported procedures. [AuCl(DMS)] was prepared according to the literature procedures.[36] Selenium and [Ni(CO)$_4$] were purchased from Strem and used as supplied. *Caution! [Ni(CO)$_4$] is a highly volatile and toxic chemical which has to be used with great caution. Prior to use it was cooled in a freezer (−40 °C) and always used as a cold liquid throughout the whole experiment. The excess of [Ni(CO)$_4$] as well as all the contaminated glassware and syringes used in this reaction were quenched thoroughly with a solution of triphenylphosphine in THF. The vacuum trap was filled with a solution of triphenylphosphine in toluene.* Glovebox manipulations were carried out using anhydrous/oxygen-free THF and DCM obtained from an MBraun SPS800 solvent purification system and anhydrous/oxygen-free pentane obtained by refluxing over P_2O_5 for several hours followed by distillation.

^{1}H NMR spectra were recorded at 300, 400, or 500 MHz, ^{13}C{^{1}H} NMR spectra at 75, 101, or 126 MHz, and ^{77}Se{^{1}H} NMR spectra at 76 or 95 MHz using Bruker Avance spectrometers. NMR spectra were referenced internally to residual solvent resonances (for ^{1}H) and solvent signals (for ^{13}C{^{1}H})[43] or externally to $(PhSe)_2$ (for ^{77}Se{^{1}H}). Chemical shifts are reported in ppm. Proton and carbon chemical shifts are reported relative to $SiMe_4$ (δ_H, δ_C 0 ppm), and selenium chemical shifts relative to $(PhSe)_2$ (δ_{Se} 463 ppm). Coupling constants are reported in Hz. Carbon and selenium resonances were singlets unless otherwise stated. IR analyses were carried out in solution cells using a Perkin-Elmer spectrometer, and frequencies are reported in wavenumbers (cm^{-1}). Elemental analyses were carried out at the London Metropolitan University and are reported as the average of two analyses.

X-ray Crystallographic Analyses. Details of the data collection and refinement can be found in the Supporting Information. X-ray diffraction data for compounds **1b**,**d**, **2d**, and **3b**,**d** were collected by using a Rigaku MM007 High brilliance RA generator/confocal optics and Mercury CCD system. Data for compound **2b** were collected by using a Rigaku MM007 High brilliance RA generator/confocal optics and Saturn CCD system. Data for compounds **1f**, **3e**,**f**, and **5c**,**d**,**f** were collected by using a Rigaku FR-X Ultrahigh brilliance Microfocus RA generator/confocal optics and Rigaku XtaLAB P200 system. Data for compounds **5a**,**b**,**e** were collected on a Rigaku SCXmini CCD system. Intensity data were collected at low temperature (173 K for **1d**, **2d**, **3b**, **5a**−**f**; 93 K for **1b**,**f**, **2b**, **3d**−**f**), using graphite-monochromated Mo Kα radiation (λ = 0.71073 Å), and ω or both ω and φ steps accumulating area detector images spanning at least a hemisphere of reciprocal space. All data were corrected for Lorentz polarization effects. A multiscan absorption correction was applied by using CrystalClear.[44] Structures were solved by Patterson (PATTY)[45] or direct methods (SHELXS97,[46] SIR97,[47] SIR2004,[48] or SIR2011)[49] and refined by full-matrix least squares against F^2 (SHELXL-2013).[46] Non-hydrogen atoms were refined anisotropically, and hydrogen atoms were refined using a riding model. All calculations were performed using the CrystalStructure interface.[50]

Synthesis of Tetrafluoroborate Salts. The NHC·HCl salt was dissolved in a 100/1 v/v water/THF mixture and stirred for 15 min. The almost clear solution was then treated with excess HBF_4 (48% w/w in water) at room temperature, which resulted in the formation of a yellowish suspension. After the mixture was stirred for a further 20 min, the solid was isolated by filtration. The yellow solid was dissolved in DCM, dried over anhydrous sodium sulfate, and filtered. The filtrate was concentrated before the addition of pentane, which caused precipitation of the pure imidazolium tetrafluoroborate salt; this was isolated by filtration and dried under vacuum.

IPr^{OMe}***·HBF***$_4$. **IPr**^{OMe}·HCl (1.95 g, 4.01 mmol, 1.0 equiv) was treated with HBF_4 solution (1.0 mL, 10.2 mmol, 2.5 equiv) to yield a pale yellowish powder (2.00 g, 3.73 mmol, 93%). ^{1}H NMR (300 MHz, $CDCl_3$): δ 8.72 (1H, t, *J* = 1.5, N(CH)N), 7.65 (2H, d, *J* = 1.4, N(C*H*)$_2$N), 6.76 (4H, s, ArH), 3.85 (6H, s, OCH_3), 2.33 (4H, sept,

dx.doi.org/10.1021/om5001919 | *Organometallics* 2014, 33, 2048−2058

$^3J_{HH}$ = 6.8 Hz, C*H*(CH_3)$_2$), 1.20 (12H, d, $^3J_{HH}$ = 6.8, CH(C*H*$_3$)$_2$), 1.13 (12H, d, $^3J_{HH}$ = 6.8, CH(C*H*$_3$)$_2$). ^{13}C{^{1}H} NMR (75 MHz, $CDCl_3$): δ 162.0 (ArC), 146.7 (ArC), 138.3 (N(CH)N), 126.8 (N(CH)$_2$N), 122.7 (ArC), 110.0 (ArCH), 55.6 (OCH_3), 29.3 (*C*H(CH$_3$)$_2$), 24.3 (CH(*C*H$_3$)$_2$), 23.8 (CH(*C*H$_3$)$_2$). Anal. Calcd for $C_{29}H_{41}BF_4N_2O_2$: C, 64.93; H, 7.70; N, 5.22; Found: C, 64.66; H, 7.77; N, 5.14.

SIPr^{OMe}·HBF$_4$. **SIPr^{OMe}**·HCl (4.00 g, 8.21 mmol, 1.0 equiv) was treated with HBF_4 (1.30 mL, 13.3 mmol, 1.6 equiv) to yield a bright white powder (4.05 g, 7.52 mmol, 92%). ^{1}H NMR (300 MHz, $CDCl_3$): δ 7.86 (1H, s, N(CH)N), 6.74 (4H, s, ArH), 4.66 (4H, s, N(CH)$_2$N), 3.84 (6H, s, OCH_3), 2.97 (4H, sept, $^3J_{HH}$ = 6.8 Hz, C*H*(CH$_3$)$_2$), 1.37 (12H, d, *J* = 6.8, CH(C*H*$_3$)$_2$), 1.22 (12H, d, *J* = 6.8, CH(C*H*$_3$)$_2$). ^{13}C{^{1}H} NMR (75 MHz, $CDCl_3$): δ 161.7 (ArC), 158.8 (N(CH)N), 148.0 (ArC), 122.1 (ArC), 110.4 (ArCH), 55.6 (N(CH$_2$)$_2$N), 55.0 (OCH_3), 29.4 (*C*H(CH$_3$)$_2$), 25.4 (CH(*C*H$_3$)$_2$), 23.9 (CH(*C*H$_3$)$_2$). Anal. Calcd for $C_{29}H_{43}BF_4N_2O_2$: C, 64.69; H, 8.05; N, 5.20; Found: C, 64.65; H, 7.95; N, 5.23.

Synthesis of Free Carbenes. Inside the glovebox, the tetrafluoroborate salt was suspended in THF and NaH was added, plus a catalytic amount (spatula tip) of KO^{t}Bu. The mixture was stirred overnight at room temperature, before removal of the solid byproducts by filtration through a pad of Celite on a frit. The mother liquor was concentrated to a fourth of the starting volume, and pentane was added. The solution was cooled to −38 °C to promote precipitation of the product. The solid was then filtered off and washed with pentane.

IPr^{OMe}. **IPr^{OMe}**·HBF_4 (1.00 g, 1.86 mmol) and NaH (50 mg, 2.0 mmol) in THF (250 mL) yielded a white solid (735 mg, 1.64 mmol, 88%). ^{1}H NMR (400 MHz, C_6D_6): δ 6.91 (4H, s, ArH), 6.67 (2H, s, N(CH)$_2$N), 3.46 (6H, s, OCH_3), 2.98 (4H, sept, $^3J_{HH}$ = 6.9, C*H*(CH$_3$)$_2$), 1.31 (12H, d, $^3J_{HH}$ = 6.9, CH(C*H*$_3$)$_2$), 1.20 (12H, d, $^3J_{HH}$ = 6.9, CH(C*H*$_3$)$_2$). ^{13}C{^{1}H} NMR (101 MHz, C_6D_6): δ 221.6 (NCN), 160.4 (ArC), 147.7 (ArC), 132.4 (ArC), 121.9 (N(CH)$_2$N), 109.1 (ArCH), 54.9 (OCH_3), 29.1 (*C*H(CH$_3$)$_2$), 24.7 (CH(*C*H$_3$)$_2$), 23.6 (CH(*C*H$_3$)$_2$).

SIPr^{OMe}. **SIPr^{OMe}**·HBF_4 (2.00 g, 3.7 mmol) and NaH (100 mg, 4.0 mmol) in THF (500 mL) yielded a white solid (1.1 g, 2.44 mmol, 66% yield). ^{1}H NMR (400 MHz, C_6D_6): δ 6.90 (4H, s, ArH), 3.46 (6H, s, OCH_3) 3.40 (4H, s, N(CH$_2$)N), 3.30 (4H, sept, $^3J_{HH}$ = 6.8, C*H*(CH$_3$)$_2$), 1.36 (12H, d, $^3J_{HH}$ = 6.8, CH(C*H*$_3$)$_2$), 1.30 (12H, d, $^3J_{HH}$ = 6.8, CH(C*H*$_3$)$_2$). ^{13}C{^{1}H} NMR (101 MHz, C_6D_6): δ 245.0 (NCN), 159.9 (ArC), 148.8 (ArC), 132.8 (ArC), 109.5 (ArCH), 54.9 (OCH_3), 53.9 (N(CH$_2$)$_2$N), 29.3 (*C*H(CH$_3$)$_2$), 25.4 (CH(*C*H$_3$)$_2$), 23.6 (CH(*C*H$_3$)$_2$).

Synthesis of [AuCl(NHC)] Complexes 1. A vial was charged, in air, with NHC·HCl, [AuCl(DMS)], and finely ground K_2CO_3. The resulting mixture was dissolved in acetone (1.0 mL) and stirred for 3 h at 60 °C. After this time, the mixture was filtered through silica, which was rinsed with dichloromethane. The solvent was concentrated, and pentane (3.0 mL) was added, which brought about precipitation of the product as a white solid; this was collected by filtration, washed with further portions of pentane (3 × 1.0 mL), and dried in vacuo.

[AuCl(IPr^{OMe})] (1b). **IPr^{OMe}**·HCl (100 mg, 0.206 mmol), [AuCl(DMS)] (60.7 mg, 0.206 mmol) and K_2CO_3 (28.5 mg, 0.206 mmol). The silica pad was rinsed with dichloromethane (3 × 1.0 mL). White solid (101 mg, 0.148 mmol, 72%). ^{1}H NMR (300 MHz, $CDCl_3$): δ 7.11 (2H, s, N(C*H*)$_2$N), 6.75 (4H, s, ArH), 3.87 (6H, s, OC*H*$_3$), 2.51 (4H, sept, $^3J_{H-H}$ = 6.8, C*H*(CH$_3$)$_2$), 1.32 (12H, d, $^3J_{H-H}$ = 6.8, CH(C*H*$_3$)$_2$), 1.19 (12H, d, $^3J_{H-H}$ = 6.9, CH(C*H*$_3$)$_2$). ^{13}C{^{1}H}-DEPTQ NMR (75 MHz, $CDCl_3$): δ 176.3 (Au−C), 161.0 (*C*-OCH$_3$), 147.2 (ArC), 127.2 (ArC), 123.5 (N(CH)$_2$N), 109.7 (ArCH), 55.5 (OCH_3), 29.1 (*C*H(CH$_3$)$_2$), 24.5 (CH(*C*H$_3$)$_2$), 24.1 (CH-(*C*H$_3$)$_2$). Anal. Calcd for $C_{29}H_{40}AuClN_2O_2$: C, 51.14; H, 5.92; N, 4.11. Found: C, 51.17; H, 5.89; N, 4.15. Crystals suitable for X-ray diffraction studies were grown by slow diffusion of pentane into a saturated dichloromethane solution.

[AuCl(SIPr^{OMe})] (1d). **SIPr^{OMe}**·HCl (100 mg, 0.205 mmol), [AuCl(DMS)] (60.5 mg, 0.205 mmol), and K_2CO_3 (28.4 mg, 0.205 mmol). The silica pad was rinsed with dichloromethane (5 × 2.0 mL). White solid (78 mg, 0.114 mmol, 56%). The low isolated yield is due to the low solubility of the complex in acetone and dichloromethane. ^{1}H NMR (500 MHz, $CDCl_3$): δ 6.71 (s, 4H, ArH), 3.99 (s, 4H, N(C*H*$_2$)$_2$N), 3.85 (s, 6H, OC*H*$_3$), 3.01 (sept, $^3J_{H-H}$ = 6.8, 4H, C*H*(CH$_3$)$_2$), 1.40 (d, $^3J_{H-H}$ = 6.8, 12H, CH(C*H*$_3$)$_2$), 1.32 (d, $^3J_{H-H}$ = 6.9, 12H, CH(C*H*$_3$)$_2$). ^{13}C{^{1}H}-DEPTQ NMR (126 MHz, $CDCl_3$): δ 197.0 (Au−C), 160.5 (*C*−OCH$_3$), 148.2 (ArC), 127.3 (ArC), 110.1 (ArCH), 55.4 (OCH_3), 53.7 (N(*C*H$_2$)$_2$N), 29.3 (*C*H(CH$_3$)$_2$), 25.2 (CH(*C*H$_3$)$_2$), 24.2 (CH(*C*H$_3$)$_2$). Anal. Calcd for $C_{29}H_{42}AuClN_2O_2$: C, 50.99; H, 6.20; N, 4.10. Found: C, 50.92; H, 6.28; N, 4.16. Crystals suitable for X-ray diffraction studies were grown by slow diffusion of pentane into a saturated dichloromethane solution.

[AuCl(IPr*^{OMe})] (1f). **IPr*^{OMe}**·HCl (100 mg, 0.102 mmol), [AuCl(DMS)] (30.0 mg, 0.102 mmol) ,and K_2CO_3 (14.1 mg, 0.102 mmol). The silica pad was rinsed with dichloromethane (3 × 1.0 mL). White solid (109 mg, 0.093 mmol, 91%). ^{1}H NMR (400 MHz, $CDCl_3$): δ 7.23−7.09 (32H, m, ArH), 6.93−6.87 (8H, m, ArH), 6.56 (4H, s, ArH), 5.76 (2H, s, N(C*H*)$_2$N), 5.27 (4H, s, C*H*Ph$_2$), 3.59 (6H, s, OC*H*$_3$). ^{13}C{^{1}H}-DEPTQ NMR (101 MHz, $CDCl_3$): δ 176.0 (Au−C), 160.2 (*C*−OCH$_3$), 142.9 (ArC), 142.8 (ArC), 142.2 (ArC), 129.7 (ArCH), 129.4 (ArCH), 129.3 (ArC), 128.7 (ArCH), 128.5 (ArCH), 126.9 (ArCH), 123.4 (N(*C*H)$_2$N), 115.2 (ArCH), 55.3 (OCH$_3$), 51.5 (CHPh$_2$). Anal. Calcd for $C_{69}H_{56}AuClN_2O_2$: C, 70.37; H, 4.79; N, 2.38. Found: C, 70.56; H, 4.76; N, 2.37. Crystals suitable for X-ray diffraction studies were grown by slow diffusion of pentane into a saturated benzene solution.

Synthesis of [Ni(CO)$_3$(NHC)] Complexes 2. In the glovebox, a −40 °C solution of free carbene in THF was treated with an excess of cold [Ni(CO)$_4$]. After 6 h at room temperature, the reddish solution was concentrated under vacuum. The resulting reddish crude solid was dissolved in DCM (3 × 3 mL) and filtered through a pad of Celite and cotton wool. The combined fractions were then concentrated under vacuum, affording the desired complex.

[Ni(CO)$_3$(IPr^{OMe})] (2b). **IPr^{OMe}** (130 mg, 0.27 mmol, 1.0 equiv) in THF (6 mL) was treated with [Ni(CO)$_4$] (100 μL, 0.77 mmol, 2.9 equiv). Light purple solid (149 mg, 0.252 mol, 93%). ^{1}H NMR (300 MHz, $CDCl_3$): δ 7.09 (2H, app d, *J* = 1.7, N(CH)$_2$N), 6.79 (4H, s, ArH), 3.87 (6H, s, OCH_3), 2.61 (4H, sept, $^3J_{HH}$ = 6.9, C*H*(CH$_3$)$_2$), 1.26 (12H, d, $^3J_{HH}$ = 6.9, CH(C*H*$_3$)$_2$), 1.13 (12H, d, $^3J_{HH}$ = 6.9, CH(C*H*$_3$)$_2$). ^{13}C{^{1}H} NMR (75 MHz, $CDCl_3$): δ 198.0 (CO), 197.4 (Ni−C), 160.5 (ArC), 147.5 (ArC), 131.0 (N(CH)$_2$N), 123.7 (ArC), 109.2 (ArC), 55.5 (OCH_3), 28.8 (CH(CH$_3$)$_2$), 25.4 (CH(*C*H$_3$)$_2$), 22.6 (CH(*C*H$_3$)$_2$). Anal. Calcd for $C_{32}H_{40}N_2NiO_5$: C, 64.99; H, 6.82; N, 4.74; Found: C, 64.82; H, 6.92; N, 4.81. IR ν_{CO} (hexane, cm^{-1}): 2053.7 (vs), 1978.3 (s), 1970.2 (s). IR ν_{CO} (CH_2Cl_2, cm^{-1}): 2049.9 (vs), 1972.9 (s), 1960.9 (s). Crystals suitable for X-ray diffraction studies were grown by slow diffusion of pentane into a benzene solution.

[Ni(CO)$_3$(SIPr^{OMe})] (2d). **SIPr^{OMe}** (130 mg, 0.27 mmol, 1.0 equiv) in THF (6 mL) was treated with [Ni(CO)$_4$] (100 μL, 0.77 mmol, 2.9 equiv). Dark purple solid (92 mg, 0.155 mmol, 57%). ^{1}H NMR (300 MHz, $CDCl_3$): δ 6.74 (4H, s, ArH), 3.92 (4H, s, N(CH$_2$)N), 3.84 (6H, s, OCH_3), 3.10 (4H, sept, $^3J_{HH}$ = 6.9, C*H*(CH$_3$)$_2$), 1.31 (12H, d, $^3J_{HH}$ = 6.9, CH(C*H*$_3$)$_2$), 1.27 (12H, d, *J* = 6.9, CH(C*H*$_3$)$_2$). ^{13}C{^{1}H} NMR (126 MHz, $CDCl_3$): δ 223.4 (Ni-C), 197.3 (CO), 159.8 (ArC), 148.5 (ArC), 131.5 (ArC), 109.6 (ArCH), 55.5 (OCH_3), 53.4 (N(CH)$_2$N), 28.7 (*C*H(CH$_3$)$_2$), 26.0 (CH(*C*H$_3$)$_2$), 23.6 (CH-(*C*H$_3$)$_2$). Anal. Calcd for $C_{32}H_{42}N_2NiO_5$: C, 64.77; H, 7.13; N, 4.72; Found: C, 64.84; H, 7.05; N, 4.78. IR ν_{CO} (hexane, cm^{-1}): 2054.1 (vs), 1980.5 (s), 1971.6 (s). IR ν_{CO} (CH_2Cl_2, cm^{-1}): 2050.3 (vs), 1973.9 (s), 1962.1 (s). Crystals suitable for X-ray diffraction studies were grown by slow diffusion of pentane into a benzene solution.

Synthesis of [IrCl(COD)(NHC)] Complexes 3. In the glovebox, a solution of free carbene in THF was added to [IrCl(COD)]$_2$, whereupon a pale yellow solution was formed. After it was stirred at room temperature, the solution gradually became darker. After the solution was stirred overnight, the solvent was stripped and the residue was worked up.

[IrCl(COD)(IPr^{OMe})] (3b). **IPr^{OMe}** (20.1 mg, 0.045 mmol) in THF (1 mL) was added to [IrCl(COD)]$_2$ (15.0 mg, 0.022 mmol, 0.50 equiv) and the mixture stirred overnight. The residue was taken up in diethyl

dx.doi.org/10.1021/om5001919 | *Organometallics* 2014, 33, 2048−2058

ether (2 mL) and filtered through a short pad of silica gel, followed by diethyl ether (3 mL). The combined fractions were evaporated to yield a sticky yellow oil, which was solidified by the addition of cold (−40 °C) pentane and scratching with a spatula. The pentane was removed in vacuo, and the resulting yellow powder was carefully washed with 0.3 mL of cold (−40 °C) pentane and dried in vacuo to yield the title compound (22.2 mg, 0.028 mmol, 63%). ^{1}H NMR (500 MHz, C_6D_6): δ 6.91 (4H, s, ArH), 6.62 (2H, s, $N(CH)_2N$), 4.80−4.64 (2H, m, COD CH), 4.08−3.83 (2H, m, $CH(CH_3)_2$), 3.36 (6H, s, OCH_3), 3.26−3.14 (2H, m, COD CH), 2.79−2.58 (2H, m, $CH(CH_3)_2$), 1.84−1.74 (4H, m, COD CH_2), 1.74−1.64 (6H, m, $CH(CH_3)_2$), 1.38−1.32 (4H, m, COD CH_2), 1.32−1.12 (6H, m, $CH(CH_3)_2$), 1.19−1.07 (6H, m, $CH(CH_3)_2$), 1.06−0.94 (6H, m, $CH(CH_3)_2$). $^{13}C\{^1H\}$ NMR (126 MHz, C_6D_6): δ 185.0 (Ir−C), 161.1 (ArC), 149.8 (ArC), 147.2 (ArC), 129.9 (ArC), 124.8 ($N(CH)_2N$), 109.5 (ArH), 109.0 (ArH), 83.3 (COD CH), 54.8 (OCH_3), 50.9 (COD CH), 34.2 (COD CH_2), 29.5 (br, $CH(CH_3)_2$), 29.2 (COD CH_2), 26.7 (br, $CH(CH_3)_2$), 26.6 (br, $CH(CH_3)_2$), 23.7 (br, $CH(CH_3)_2$), 22.5 (br, $CH(CH_3)_2$). Anal. Calcd for $C_{37}H_{52}N_2IrO_2$: C, 56.65; H, 6.68; N, 3.57. Found: C, 56.80; H, 6.63; N, 3.50. Crystals suitable for X-ray diffraction studies were grown by slow diffusion of pentane into a diethyl ether solution.

*[IrCl(COD)(**SIPr^{OMe}**)] (**3d**).* **SIPr^{OMe}** (20.4 mg, 0.0453 mmol) in THF (1 mL) was added to $[IrCl(COD)]_2$ (15.0 mg, 0.0223 mmol, 0.50 equiv) and the mixture stirred overnight. The residue was taken up in diethyl ether (2 mL) and filtered through a short pad of silica gel, followed by the addition of diethyl ether (3 mL). The combined fractions were evaporated in vacuo to yield a sticky yellow oil, which was solidified by the addition of cold (−40 °C) pentane and scratching with a spatula. The pentane was removed in vacuo, and the resulting yellow powder was carefully washed with 0.3 mL of cold (−40 °C) pentane and dried in vacuo to yield the title compound (23.7 mg, 0.030 mmol, 66%). ^{1}H NMR (500 MHz, C_6D_6): δ 6.91 (2H, d, $^3J_{HH}$ = 2.8, ArH), 6.89 (2H, d, $^3J_{HH}$ = 2.8, ArH), 4.75−4.64 (2H, m, COD CH), 4.28 (2H, sept, $^2J_{HH}$ = 6.8 Hz, $CH(CH_3)_2$), 3.74−3.68 (2H, m, $N(CH_2)_2N$), 3.51−3.46 (2H, m, $N(CH_2)_2N$), 3.38 (6H, s, OCH_3), 3.29−3.11 (4H, m, COD CH and $CH(CH_3)_2$), 1.78 (6H, d, $^2J_{HH}$ = 6.8 Hz, $CH(CH_3)_2$), 1.74−1.62 (4H, m, COD CH_2), 1.36 (6H, d, $^2J_{HH}$ = 6.8 Hz, $CH(CH_3)_2$), 1.32−1.24 (4H, m, COD CH_2), 1.22 (6H, d, $^2J_{HH}$ = 6.8 Hz, $CH(CH_3)_2$), 1.10 (6H, d, $^2J_{HH}$ = 6.8 Hz, $CH(CH_3)_2$). $^{13}C\{^1H\}$ NMR (126 MHz, C_6D_6): δ 211.2 (Ir−C), 160.5 (ArC), 151.2 (ArC), 147.9 (ArC), 130.4 (ArC), 110.0 (ArH), 109.4 (ArH), 84.0 (COD CH), 54.8 (OCH_3), 54.4 ($N(CH_2)_2N$), 50.9 (COD CH), 29.5 ($CH(CH_3)_2$), 29.4 ($CH(CH_3)_2$), 28.9 (COD CH_2), 27.1 ($CH(CH_3)_2$), 26.9 ($CH(CH_3)_2$), 24.6 ($CH(CH_3)_2$), 23.2 ($CH(CH_3)_2$). Anal. Calcd for $C_{37}H_{54}N_2IrO_2$: C, 56.50; H, 6.92; N, 3.56. Found: C, 56.63; H, 6.83; N, 3.53. Crystals suitable for X-ray diffraction studies were grown by slow evaporation of a diethyl ether solution.

[IrCl(COD)(IPr)] (**3e**).* **IPr*** (224.7 mg, 0.246 mmol, 2.2 equiv) and $[IrCl(COD)]_2$ (75.7 mg, 0.113 mmol) in THF (3.5 mL), stirred for 36 h (time not optimized). The residue was dissolved in ethyl acetate (5 mL) and filtered through a pad of silica, which was washed with ethyl acetate (10 mL). The solvent was removed in vacuo, and the resulting residue was dissolved in benzene and filtered using a syringe filter. The benzene was removed in vacuo, and the resulting yellow powder was washed with pentane and dried under high vacuum to yield the title complex (243.0 mg, 0.195 mmol, 86%). ^{1}H NMR (500 MHz, $CDCl_3$): δ 7.66−7.54 (4H, m, ArH), 7.39−7.19 (16H, m, ArH), 7.19−7.00 (12H, m, ArH), 6.95 (2H, s, ArH), 6.90 (2H, s, ArH), 6.85−6.78 (4H, m, ArH), 6.76−6.69 (4H, m, ArH), 6.50 (2H, s, $CHPh_2$), 5.70 (2H, s, $CHPh_2$), 4.97 (2H, s, $N(CH)_2N$), 4.82−4.76 (2H, m, COD CH), 3.37−3.29 (2H, m, COD CH), 2.29 (6H, s, OCH_3), 2.20−2.09 (2H, m, COD CH_2), 1.79−1.68 (2H, m, COD CH_2), 1.68−1.59 (2H, m, COD CH_2), 1.34−1.24 (2H, m, COD CH_2). $^{13}C\{^1H\}$ NMR (126 MHz, $CDCl_3$): δ 178.8 (Ir−C), 144.6 (ArC), 144.4 (ArC), 143.9 (ArC), 143.7 (ArC), 143.2 (ArC), 140.7 (ArC), 138.1 (ArC), 136.4 (ArC), 131.0 (ArCH), 130.9 (ArCH), 130.2 (ArCH), 129.7 (ArCH), 129.7 (ArCH), 129.3 (ArCH), 128.3 (ArCH), 128.1 (ArCH), 127.8 (ArCH), 126.5 (ArCH), 126.0 (ArCH), 126.0 (ArCH), 123.7 ($N(CH)_2N$), 83.7 (COD CH), 53.2 (COD CH), 51.4 ($CHPh_2$), 51.0 ($CHPh_2$), 33.4 (COD CH_2), 28.9 (COD CH_2), 21.9 ($ArCH_3$). Anal. Calcd for $C_{37}H_{54}N_2IrO_2$: C, 74.04; H, 5.49; N, 2.24. Found: C, 74.23; H, 5.68; N, 2.37. Crystals suitable for X-ray diffraction studies were grown by slow diffusion of pentane into a benzene solution.

[IrCl(COD)(IPr^{OMe})] (**3f**).* **IPr*^{OMe}** (102.5 mg, 0.108 mmol, 2.1 equiv) and $[IrCl(COD)]_2$ (35.0 mg, 0.052 mmol) in THF (3 mL), stirred overnight. The residue was washed with diethyl ether (3 × 1 mL) and pentane (3 × 1 mL) and dried in vacuo to yield a yellow powder (105.8 mg, 0.083 mmol, 79%). ^{1}H NMR (500 MHz, $CDCl_3$): δ 7.55−6.48 (44H, m, ArH), 6.44 (2H, s, $CHPh_2$), 5.54 (2H, s, $CHPh_2$), 4.80 (2H, s, $N(CH)_2N$), 4.70−4.63 (2H, m, COD CH), 3.56 (6H, s, OCH_3), 3.29−3.22 (2H, m, COD CH), 2.11−1.99 (2H, m, COD CH_2), 1.72−1.61 (2H, m, COD CH_2), 1.60−1.50 (2H, m, COD CH_2), 1.33−1.18 (2H, m, COD CH_2). $^{13}C\{^1H\}$ NMR (126 MHz, $CDCl_3$): 179.7 (Ir−C), 158.8 (ArC), 145.3 (ArC), 144.4 (ArC), 144.1 (ArC), 143.7 (ArC), 143.5 (ArC), 142.5 (ArC), 131.9 (ArC), 130.9 (ArCH), 130.2 (ArCH), 129.6 (ArCH), 129.3 (ArCH), 128.3 (ArCH), 128.2 (ArCH), 128.1 (ArCH), 127.9 (ArCH), 126.7 (ArCH), 126.6 (ArCH), 126.2 (ArCH), 126.1 (ArCH), 123.7 ($N(CH)_2N$), 115.4 (ArCH), 114.6 (ArCH), 83.7 (COD CH), 55.2 (OCH_3), 53.1 (COD CH), 51.7 ($CHPh_2$), 51.3 ($CHPh_2$), 33.5 (COD CH_2), 28.9, (COD CH_2). Anal. Calcd for $C_{77}H_{68}N_2IrClO_2$: C, 72.19; H, 5.35; N, 2.19. Found: C, 71.77; H, 5.20; N, 2.43. Crystals suitable for X-ray diffraction studies were grown by slow diffusion of pentane into a benzene solution.

Synthesis of [IrCl(CO)$_2$(NHC)] Complexes 4. The corresponding [IrCl(COD)(NHC)] complex (**3**) was dissolved in DCM and exposed to carbon monoxide (**4b** in a Schlenk flask, avoiding air and moisture; **4d**−**f** in vials). Over this time, the reaction turned from dark golden yellow to a pale straw yellow. The solvent was then removed in vacuo, and the residue was washed with pentane and dried in vacuo.

*[IrCl(CO)$_2$(IPr^{OMe})] (**4b**).* **3b** (30.2 mg, 0.0385 mmol) was dissolved in DCM (2.5 mL) in a flask fitted with a J. Young tap. The flask was removed from the glovebox, the solution was frozen, and the headspace was evacuated. The flask was then filled with carbon monoxide and stirred at room temperature for 6 h. The flask was placed under static vacuum and reintroduced into the glovebox. The residue was washed with cold (−40 °C) pentane (3 × 0.3 mL) and dried in vacuo to yield a pale yellow powder (19.1 mg, 0.026 mmol, 68%). ^{1}H NMR (300 MHz, C_6D_6): δ 6.86 (4H, s, ArH), 6.62 (2H, s, $N(CH)_2N$), 3.30 (6H, s, OCH_3), 3.13 (4H, sept, $^2J_{HH}$ = 6.7, $CH(CH_3)_2$), 1.51 (12H, d, $^3J_{HH}$ = 6.7, $CH(CH_3)_2$), 1.05 (12H, d, $^3J_{HH}$ = 6.7, $CH(CH_3)_2$). $^{13}C\{^1H\}$ NMR (75 MHz, C_6D_6): δ 180.8 (CO), 180.4 (Ir−C), 169.9 (CO), 161.6 (ArC), 147.9 (ArC), 128.0 (ArC), 125.1 ($N(CH)_2N$), 109.8 (ArCH), 54.8 (OCH_3), 29.5 ($CH(CH_3)_2$), 26.4 ($CH(CH_3)_2$), 22.8 ($CH(CH_3)_2$). [^{1}H, ^{13}C] HMBC was used to locate the signal at 128.0 ppm and to assign the $C_{carbene}$ signal. Anal. Calcd for $C_{31}H_{40}N_2ClIrO_4$: C, 50.84; H, 5.51; N, 3.83. Found: C, 50.96; H, 5.33; N, 3.98. IR ν_{CO} (CH_2Cl_2, cm^{-1}): 2066.3 (vs), 1980.4 (vs).

*[IrCl(CO)$_2$(SIPr^{OMe})] (**4d**).* **3d** (26.4 mg, 0.034 mmol) in DCM (1.5 mL) was sparged with CO for ca. 5 min. The reaction mixture was stirred overnight under a balloon of CO. The residue was washed with pentane (3 × 1 mL) and dried in vacuo to yield a pale yellow powder (17.8 mg, 0.0247 mmol, 72%). ^{1}H NMR (300 MHz, $CDCl_3$): δ 6.76 (4H, s, ArH), 4.03 (4H, s, $N(CH_2)_2N$), 3.86 (6H, s, OCH_3), 3.34 (2H, sept, $^3J_{HH}$ = 6.8, $CH(CH_3)_2$), 1.44 (6H, d, $^3J_{HH}$ = 6.8, $CH(CH_3)_2$), 1.27 (6H, d, $^3J_{HH}$ = 6.8, $CH(CH_3)_2$). $^{13}C\{^1H\}$ NMR (75 MHz, $CDCl_3$): δ 205.4 (Ir−C), 180.4 (CO), 168.8 (CO), 160.1 (ArC), 148.7 (ArC), 128.1 (ArC), 109.8 (ArCH), 55.3 (OCH_3), 54.6 ($N(CH_2)_2N$), 29.2 ($CH(CH_3)_2$), 26.9 ($CH(CH_3)_2$), 23.6 ($CH(CH_3)_2$). Anal. Calcd for $C_{31}H_{40}N_2ClIrO_4$: C, 50.70; H, 5.77; N, 3.81. Found: C, 50.62; H, 5.86; N, 3.74. IR ν_{CO} (CH_2Cl_2, cm^{-1}): 2067.2 (vs), 1981.6 (vs).

[IrCl(CO)$_2$(IPr)] (**4e**).* **3e** (75.1 mg, 0.060 mmol) in DCM (3 mL) was sparged with CO for ca. 10 min. The residue was washed with pentane (3 × 1 mL) and dried under high vacuum to yield a pale yellow solid (65.8 mg, 0.055 mmol, 92%). ^{1}H NMR (500 MHz, $CDCl_3$): δ 7.38−7.21 (20H, m, ArH), 7.14−7.05 (12H, m, ArH), 6.80 (4H, s, ArH), 6.77−6.73 (8H, m, ArH), 5.90 (4H, s, $CHPh_2$), 5.02 (2H, s, $N(CH)_2N$), 2.23 (6H, s, CH_3). $^{13}C\{^1H\}$ NMR (126 MHz,

dx.doi.org/10.1021/om5001919 | Organometallics 2014, 33, 2048−2058

$CDCl_3$): δ 179.8 (CO), 176.0 (C−Ir), 168.0 (CO), 144.3 (ArC), 143.3 (ArC), 141.4 (ArC), 139.1 (ArC), 134.6 (ArC), 130.6 (ArCH), 130.5 (ArCH), 129.3 (ArCH), 128.4 (ArCH), 128.2 (ArCH), 126.6 (ArCH), 126.5 (ArCH), 123.5 ($N(CH)_2N$), 51.7 ($CHPh_2$), 22.0 (CH_3). IR ν_{CO} (CH_2Cl_2, cm^{-1}): 2067.6 (vs), 1983.6 (vs). Anal. Calcd for $C_{71}H_{56}ClN_2O_2Ir$: C, 71.25; H, 4.72; N, 2.34. Found: C, 71.37; H, 4.88; N, 2.41.

[IrCl(CO)$_2$(IPr^{OMe})] (**4f**).* **3f** (38.3 mg, 0.030 mmol) in DCM (2 mL) was sparged with CO for ca. 10 min. The residue was washed with pentane (3 × 0.5 mL) and dried in vacuo to yield a pale yellow solid (33.7 mg, 0.027 mmol, 92%). ^1H NMR (500 MHz, $CDCl_3$): δ 7.37−7.17 (20H, m, ArH), 7.15−7.06 (12H, m, ArH), 6.78 (8H, app d, J = 7.0, ArH), 6.50 (4H, s, ArH), 5.90 (4H, s, $CHPh_2$), 4.95 (2H, s, $N(CH)_2N$), 3.57 (6H, s, OCH_3). $^{13}C\{^1H\}$ NMR (126 MHz, $CDCl_3$): 179.8 (CO), 176.4 (Ir−C), 168.1 (CO), 159.3 (ArC), 144.0 (ArC), 143.4 (ArC), 143.1 (ArCH), 130.6 (ArCH), 129.2 (ArCH), 128.4 (ArCH), 128.3 (ArCH), 126.7 (ArCH), 126.5 (ArCH), 123.5 ($N(CH)_2N$), 115.2 (ArCH), 55.1 (OCH_3), 51.9 ($CHPh_2$). IR ν_{CO} (CH_2Cl_2, cm^{-1}): 2067.4 (vs), 1983.2 (vs). Anal. Calcd for $C_{71}H_{56}N_2IrClO_4$: C, 69.39; H, 4.59; N, 2.28. Found: C, 69.24; H, 4.47; N, 2.15.

Synthesis of Selenoureas 5. In the glovebox, a solution of free carbene in THF was prepared. Outside the glovebox, under argon, this THF solution was transferred onto excess selenium, and the mixture was stirred overnight at room temperature. After this time, the THF was removed, the residue was dissolved in DCM, and this solution was passed through a pad of Celite. The pad was washed with further DCM. The solvent was removed and the residue was washed with pentane or hexane (2 × 1 mL) and dried in vacuo.

*[Se(IPr)] (**5a**).* **IPr** (102.4 mg, 0.264 mmol) was in THF (10 mL) added to selenium (59.5 mg, 0.754 mmol, 2.9 equiv). White solid (118.2 mg, 0.253 mmol, 96%). ^1H NMR (500 MHz, $CDCl_3$): δ 7.48 (2H, t, $^3J_{HH}$ = 7.9, ArH), 7.31 (4H, d, $^3J_{HH}$ = 7.9, ArH), 7.01 (2H, s, $N(CH)_2N$), 2.69 (4H, sept, $^3J_{HH}$ = 6.9, $CH(CH_3)_2$), 1.34 (12H, d, $^3J_{HH}$ = 6.9, $CH(CH_3)_2$), 1.20 (12H, d, $^3J_{HH}$ = 6.9, $CH(CH_3)_2$). $^{13}C\{^1H\}$ NMR (126 MHz, $CDCl_3$): δ 162.2 (CSe), 146.2 (ArCH), 134.5 (ArC), 130.3 (ArC), 124.4 ($N(CH)_2N$), 121.2 (ArCH), 29.1 ($CH(CH_3)_2$), 24.5 ($CH(CH_3)_2$), 23.5 ($CH(CH_3)_2$). $^{77}Se\{^1H\}$ NMR (95 MHz, $CDCl_3$): δ 90.4. ^1H NMR (400 MHz, acetone-d_6): δ 7.47 (2H, s, $N(CH)_2N$), 7.47 (2H, t, $^3J_{HH}$ = 7.9, ArH), 7.33 (4H, d, $^3J_{HH}$ = 7.9, ArH), 2.75 (4H, sept, $^3J_{HH}$ = 6.9, $CH(CH_3)_2$), 1.30 (12H, d, $^3J_{HH}$ = 6.9, $CH(CH_3)_2$), 1.19 (12H, d, $^3J_{HH}$ = 6.9, $CH(CH_3)_2$). $^{77}Se\{^1H\}$ NMR (76 MHz, acetone-d_6): δ 86.7. Anal. Calcd for $C_{27}H_{36}N_2Se$: C, 69.36; H, 7.76; N, 5.99. Found: C, 69.17; H, 7.88; N, 5.93. Crystals suitable for X-ray diffraction analysis were grown by slow diffusion of pentane into an acetone solution. Data are consistent with those reported by Ganter and co-workers.[15]

*[Se(IPr^{OMe})] (**5b**).* **IPr^{OMe}** (100.2 mg, 0.223 mmol) was in THF (15 mL) added to selenium (64.2 mg, 0.813 mmol, 3.6 equiv). Salmon-colored solid (104.2 mg, 0.197 mmol, 89%). ^1H NMR (500 MHz, $CDCl_3$): δ 6.97 (2H, s, $N(CH)_2N$), 6.80 (4H, s, ArH), 3.86 (6H, s, OCH_3), 2.65 (4H, sept, $^3J_{HH}$ = 6.9, $CH(CH_3)_2$), 1.33 (12H, d, $^3J_{HH}$ = 6.9, $CH(CH_3)_2$), 1.19 (12H, d, $^3J_{HH}$ = 6.9, $CH(CH_3)_2$). $^{13}C\{^1H\}$ NMR (126 MHz, $CDCl_3$): δ 163.0 (CSe), 160.59 (ArC), 147.6 (ArC), 127.7 (ArC), 121.4 ($N(CH)_2N$), 109.7 (ArH), 55.3 (OCH_3), 29.3 ($CH(CH_3)_2$), 24.4 ($CH(CH_3)_2$), 23.4 ($CH(CH_3)_2$). ^1H NMR (500 MHz, acetone-d_6): δ 7.39 (2H, s, $N(CH)_2N$), 6.84 (4H, s, ArH), 3.87 (6H, s, OCH_3), 2.70 (4H, sept, $^3J_{HH}$ = 6.9, $CH(CH_3)_2$), 1.29 (12H, d, $^3J_{HH}$ = 6.9, $CH(CH_3)_2$), 1.18 (12H, d, $^3J_{HH}$ = 6.9, $CH(CH_3)_2$). $^{77}Se\{^1H\}$ NMR (95 MHz, acetone-d_6): δ 83.4. Anal. Calcd for $C_{29}H_{40}N_2O_2Se$: C, 66.02; H, 7.64; N, 5.31. Found: C, 65.89; H, 7.75; N, 5.21. Crystals suitable for X-ray diffraction analysis were grown by slow diffusion of pentane into an acetone solution.

*[Se(SIPr)] (**5c**).* **SIPr** (109.8 mg, 0.281 mmol) was in THF (10 mL) added to selenium (74.1 mg, 0.938 mmol, 3.3 equiv). White solid (86.7 mg, 0.185 mmol, 66%). ^1H NMR (500 MHz, $CDCl_3$): δ 7.43 (2H, t, $^3J_{HH}$ = 7.7, ArH), 7.27 (4H, d, $^3J_{HH}$ = 7.7, ArH), 4.05 (4H, s, $N(CH_2)_2N$), 3.08 (4H, sept, $^3J_{HH}$ = 6.9, $CH(CH_3)_2$), 1.40 (12H, d, $^3J_{HH}$ = 6.9, $CH(CH_3)_2$), 1.34 (12H, d, $^3J_{HH}$ = 6.9, $CH(CH_3)_2$). $^{13}C\{^1H\}$ NMR (126 MHz, $CDCl_3$): δ 184.2 (CSe), 147.3 (ArC), 135.4 (ArC), 129.5 (ArCH), 124.6 (ArCH), 51.5 ($N(CH_2)_2N$), 29.3 ($CH(CH_3)_2$), 24.9 ($CH(CH_3)$), 24.5 ($CH(CH_3)_2$). $^{77}Se\{^1H\}$ NMR (95 MHz, $CDCl_3$): δ 189.5. ^1H NMR (400 MHz, acetone-d_6): δ 7.43−7.36 (2H, m, ArH), 7.31−7.26 (4H, m, ArH), 4.16 (4H, s, $N(CH_2)_2N$), 3.21 (4H, sept, $^3J_{HH}$ = 6.9, $CH(CH_3)_2$), 1.38 (12H, d, $^3J_{HH}$ = 6.9, $CH(CH_3)_2$), 1.33 (12H, d, $^3J_{HH}$ = 6.9, $CH(CH_3)_2$). $^{77}Se\{^1H\}$ NMR (75 MHz, acetone-d_6): δ 181.1. Anal. Calcd for $C_{27}H_{38}N_2Se$: C, 69.06; H, 8.16; N, 5.97. Found: C, 68.94; H, 8.16; N, 5.98. Crystals suitable for X-ray diffraction analysis were grown by slow diffusion of pentane into an acetone solution. Data are consistent with that reported by Ganter and co-workers.[15]

*[Se(SIPr^{OMe})] (**5d**).* **SIPr^{OMe}** (85.2 mg, 0.189 mmol) was in THF (15 mL) added to selenium (70.2 mg, 0.889 mmol, 4.7 equiv). Off-white solid (78.5 mg, 0.148 mmol, 78%). ^1H NMR (500 MHz, $CDCl_3$): δ 6.76 (4H, s, ArH), 3.98 (4H, s, $N(CH_2)_2N$), 3.84 (6H, s, OCH_3), 3.01 (4H, sept, $^3J_{HH}$ = 6.9, $CH(CH_3)_2$), 1.38 (12H, d, $^3J_{HH}$ = 6.9, $CH(CH_3)_2$), 1.31 (12H, d, $^3J_{HH}$ = 6.9, $CH(CH_3)_2$). $^{13}C\{^1H\}$ NMR (126 MHz, $CDCl_3$): δ 185.0 (CSe), 159.9 (ArC), 148.6 (ArC), 128.6 (ArC), 109.9 (ArH), 55.2 (OCH_3), 51.5 ($N(CH_2)_2N$), 29.4 ($CH(CH_3)_2$), 24.8 ($CH(CH_3)_2$), 24.4 ($CH(CH_3)_2$). ^1H NMR (500 MHz, acetone-d_6): δ 6.78 (4H, s, ArH), 4.06 (4H, s, $N(CH_2)_2N$), 3.83 (6H, s, OCH_3), 3.12 (4H, sept, $^3J_{HH}$ = 6.9, $CH(CH_3)_2$), 1.34 (12H, d, $^3J_{HH}$ = 6.9, $CH(CH_3)_2$), 1.28 (12H, d, $^3J_{HH}$ = 6.9, $CH(CH_3)_2$). $^{77}Se\{^1H\}$ NMR (95 MHz, acetone-d_6): δ 176.8. Anal. Calcd for $C_{29}H_{42}N_2O_2Se$: C, 65.77; H, 7.99; N, 5.29. Found: C, 65.57; H, 8.11; N, 5.21. Crystals suitable for X-ray diffraction analysis were grown by slow diffusion of pentane into an acetone solution.

[Se(IPr)] (**5e**).* **IPr*** (200.1 mg, 0.219 mmol) was in THF (15 mL) added to selenium (52.8 mg, 0.669 mmol, 3.1 equiv). Beige solid (168.7 mg, 0.170 mmol, 78%). ^1H NMR (500 MHz, $CDCl_3$): δ 7.42−7.37 (8H, m, ArH), 7.25−7.20 (8H, m, ArH), 7.20−7.14 (4H, m, ArH), 7.13−7.07 (12H, m, ArH), 6.86 (4H, s, ArH), 6.85−6.80 (8H, m, ArH), 5.43 (4H, s, $CHPh_2$), 5.37 (2H, s, $N(CH)_2N$), 2.22 (6H, s, CH_3). $^{13}C\{^1H\}$ NMR (126 MHz, $CDCl_3$): δ 160.9 (CSe), 143.5 (ArC), 142.9 (ArC), 141.6 (ArC), 139.6 (ArC), 133.9 (ArCH), 130.4 (ArCH), 130.2 (ArCH), 129.5 (ArCH), 128.3 (ArCH), 128.2 (ArCH), 126.6 (ArCH), 126.4 (ArCH), 121.0 ($N(CH)_2N$), 51.8 ($CHPh_2$), 22.0 ($ArCH_3$). $^{77}Se\{^1H\}$ NMR (95 MHz, $CDCl_3$): δ 105.8. Anal. Calcd for $C_{69}H_{x56}N_2Se$: C, 83.53; H, 5.69; N, 2.82. Found: C, 83.38; H, 5.75; N, 2.91. Crystals suitable for X-ray diffraction analysis were grown by slow diffusion of pentane into an acetone solution.

[Se(IPr^{OMe})] (**5f**).* **IPr*^{OMe}** (165.1 mg, 0.175 mmol) was in THF (10 mL) added to selenium (56.5 mg, 0.716 mmol, 4.1 equiv). Beige solid (155.4 mg, 0.152 mmol, 87%). ^1H NMR (500 MHz, $CDCl_3$): δ 7.46−7.39 (8H, m, ArH), 7.30−7.09 (34H, m, ArH), 6.92−6.85 (8H, m, ArH), 6.61 (4H, s, ArH), 5.46 (4H, s, $CHPh_2$), 5.36 (2H, s, $N(CH)_2N$), 3.60 (6H, s, OCH_3). $^{13}C\{^1H\}$ NMR (126 MHz, $CDCl_3$): δ 161.7 (CSe), 159.8 (ArC), 143.5 (ArC), 143.3 (ArC), 142.6 (ArC), 130.1 (ArCH), 129.4 (ArCH), 128.4 (ArCH), 128.2 (ArCH), 126.7 (ArCH), 126.5 (ArCH), 121.1 ($N(CH)_2N$), 115.1 (ArCH), 55.2 (OCH_3), 52.0 ($CHPh_2$). $^{77}Se\{^1H\}$ NMR (95 MHz, $CDCl_3$): δ 103.9. Anal. Calcd for $C_{69}H_{56}N_2O_2Se$: C, 80.92; H, 5.51; N, 2.74. Found: C, 80.68; H, 5.40; N, 2.61. Crystals suitable for X-ray diffraction analysis were grown by slow diffusion of pentane into an acetone solution.

■ ASSOCIATED CONTENT

Supporting Information

Figures, tables, and CIF files giving NMR spectra for new complexes, crystallographic data for **1b,d,f**, **2b,d**, **3b,d−f**, and **5a−f**, steric maps for **1**, **2**, and **4**, and buried volumes for **5**. This material is available free of charge via the Internet at http://pubs.acs.org. Crystallographic data for CCDC 987701−987715 (**1b,d,f**, **2b,d**, **3b,d−f**, **5a−f**) can be obtained free of charge from The Cambridge Crystallographic Data Centre via www.ccdc.cam.ac.uk/data_request/cif.

AUTHOR INFORMATION

Corresponding Author

*E-mail for S.P.N.: snolan@st-andrews.ac.uk.

Notes

The authors declare no competing financial interest.

ACKNOWLEDGMENTS

We thank the ERC (Advanced Investigator Award "FUNCAT" to S.P.N.) and the EPSRC for funding. S.P.N. is a Royal Society Wolfson Merit Award Holder. Umicore are thanked for gifts of auric acid and $[IrCl(COD)]_2$.

ABBREVIATIONS

COD, 1,5-cyclooctadiene; DMS, dimethyl sulfide; **IHept**, 1,3-bis(2,6-diisoheptylphenyl)imidazol-2-ylidene; **IHept^{OMe}**, 1,3-bis(2,6-diisoheptyl-4-methoxyphenyl)imidazol-2-ylidene; **IMes**, 1,3-bis(2,4,6-trimethylphenyl)imidazol-2-ylidene; **INon**, 1,3-bis(2,6-diisononylphenyl)imidazol-2-ylidene; **INon^{OMe}**, 1,3-bis-(2,6-diisononyl-4-methoxyphenyl)imidazol-2-ylidene; **IPent**, 1,3-bis(2,6-diisopentylphenyl)imidazol-2-ylidene; **IPent^{OMe}**, 1,3-bis(2,6-diisopentyl-4-methoxyphenyl)imidazol-2-ylidene; **IPr**, 1,3-bis(2,6-diisopropylphenyl)imidazol-2-ylidene; **IPr^{OMe}**, 1,3-bis(2,6-diisopropyl-4-methoxyphenyl)imidazol-2-ylidene; **IPr***, 1,3-bis(2,6-diphenylmethyl-4-methylphenyl)imidazol-2-ylidene; **IPr*^{OMe}**, 1,3-bis(2,6-diphenylmethyl-4-methoxyphenyl)imidazol-2-ylidene; **SIMes**, 1,3-bis(2,4,6-trimethylphenyl)-4,5-dihydroimidazol-2-ylidene; **SIPr**, 1,3-bis(2,6-diisopropylphenyl)-4,5-dihydroimidazol-2-ylidene; **SIPr^{OMe}**, 1,3-bis(2,6-diisopropyl-4-methoxyphenyl)-4,5-dihydroimidazol-2-ylidene

REFERENCES

(1) Díez-González, S.; Marion, N.; Nolan, S. P. *Chem. Rev.* **2009**, *109*, 3612.
(2) Herrmann, W. A. *Angew. Chem., Int. Ed.* **2002**, *41*, 1290.
(3) Samojlowicz, C.; Bieniek, M.; Grela, K. *Chem. Rev.* **2009**, *109*, 3708.
(4) Vougioukalakis, G. C.; Grubbs, R. H. *Chem. Rev.* **2009**, *110*, 1746.
(5) Fortman, G. C.; Nolan, S. P. *Chem. Soc. Rev.* **2011**, *40*, 5151.
(6) Clavier, H.; Nolan, S. P. *Chem. Commun.* **2010**, *46*, 841.
(7) Tolman, C. A. *Chem. Rev.* **1977**, *77*, 313.
(8) Dorta, R.; Stevens, E. D.; Scott, N. M.; Costabile, C.; Cavallo, L.; Hoff, C. D.; Nolan, S. P. *J. Am. Chem. Soc.* **2005**, *127*, 2485.
(9) Nelson, D. J.; Nolan, S. P. *Chem. Soc. Rev.* **2013**, *42*, 6723.
(10) Dröge, T.; Glorius, F. *Angew. Chem., Int. Ed.* **2010**, *49*, 6940.
(11) Kelly, R. A., III; Clavier, H.; Giudice, S.; Scott, N. M.; Stevens, E. D.; Bordner, J.; Samardjiev, I.; Hoff, C. D.; Cavallo, L.; Nolan, S. P. *Organometallics* **2007**, *27*, 202.
(12) Wolf, S.; Plenio, H. *J. Organomet. Chem.* **2009**, *694*, 1487.
(13) Fantasia, S.; Petersen, J. L.; Jacobsen, H.; Cavallo, L.; Nolan, S. P. *Organometallics* **2007**, *26*, 5880.
(14) Back, O.; Henry-Ellinger, M.; Martin, C. D.; Martin, D.; Bertrand, G. *Angew. Chem., Int. Ed.* **2013**, *52*, 2939.
(15) Liske, A.; Verlinden, K.; Buhl, H.; Schaper, K.; Ganter, C. *Organometallics* **2013**, *32*, 5269.
(16) Poater, A.; Cosenza, B.; Correa, A.; Giudice, S.; Ragone, F.; Scarano, V.; Cavallo, L. *Eur. J. Inorg. Chem.* **2009**, *2009*, 1759.
(17) Benhamou, L.; Chardon, E.; Lavigne, G.; Bellemin-Laponnaz, S.; César, V. *Chem. Rev.* **2011**, *111*, 2705.
(18) Leuthäußer, S.; Schwarz, D.; Plenio, H. *Chem. Eur. J.* **2007**, *13*, 7195.
(19) Sussner, M.; Plenio, H. *Chem. Commun.* **2005**, 5417.
(20) Leuthäußer, S.; Schmidts, V.; Thiele, C. M.; Plenio, H. *Chem. Eur. J.* **2008**, *14*, 5465.
(21) Credendino, R.; Falivene, L.; Cavallo, L. *J. Am. Chem. Soc.* **2012**, *134*, 8127.
(22) Munz, D.; Allolio, C.; Döring, K.; Poethig, A.; Doert, T.; Lang, H.; Straßner, T. *Inorg. Chim. Acta* **2012**, *392*, 204.
(23) Organ, M. G.; Çalimsiz, S.; Sayah, M.; Hoi, K. H.; Lough, A. J. *Angew. Chem., Int. Ed.* **2009**, *48*, 2383.
(24) Meiries, S.; Le Duc, G.; Chartoire, A.; Collado, A.; Speck, K.; Athukorala Arachige, K. S.; Slawin, A. M. Z.; Nolan, S. P. *Chem. Eur. J.* **2013**, *19*, 17358.
(25) Meiries, S.; Speck, K.; Cordes, D. B.; Slawin, A. M. Z.; Nolan, S. P. *Organometallics* **2012**, *32*, 330.
(26) Bastug, G.; Nolan, S. P. *Organometallics* **2014**, *33*, 1253.
(27) Bastug, G.; Nolan, S. P. *J. Org. Chem.* **2013**, *78*, 9303.
(28) Le Duc, G.; Meiries, S.; Nolan, S. P. *Organometallics* **2013**, *32*, 7547.
(29) Arduengo, A. J., III; Krafczyk, R.; Schmutzler, R.; Craig, H. A.; Goerlich, J. R.; Marshall, W. J.; Unverzagt, M. *Tetrahedron* **1999**, *55*, 14523.
(30) Huang, J.; Nolan, S. P. *J. Am. Chem. Soc.* **1999**, *121*, 9889.
(31) Gómez-Suárez, A.; Ramón, R. S.; Songis, O.; Slawin, A. M. Z.; Cazin, C. S. J.; Nolan, S. P. *Organometallics* **2011**, *30*, 5463.
(32) Meiries, S.; Nolan, S. P. *Synlett* **2014**, *25*, 393.
(33) Collado, A.; Gomez-Suarez, A.; Martin, A. R.; Slawin, A. M. Z.; Nolan, S. P. *Chem. Commun.* **2013**, *49*, 5541.
(34) Fructos, M. R.; Belderrain, T. R.; de Frémont, P.; Scott, N. M.; Nolan, S. P.; Díaz-Requejo, M. M.; Pérez, P. J. *Angew. Chem., Int. Ed.* **2005**, *44*, 5284.
(35) de Frémont, P.; Scott, N. M.; Stevens, E. D.; Nolan, S. P. *Organometallics* **2005**, *24*, 2411.
(36) Hooper, T. N.; Butts, C. P.; Green, M.; Haddow, M. F.; McGrady, J. E.; Russell, C. A. *Chem. Eur. J.* **2009**, *15*, 12196.
(37) Balogh, J.; Slawin, A. M. Z.; Nolan, S. P. *Organometallics* **2012**, *31*, 3259.
(38) Chianese, A. R.; Li, X.; Janzen, M. C.; Faller, J. W.; Crabtree, R. H. *Organometallics* **2003**, *22*, 1663.
(39) Collado, A.; Balogh, J.; Meiries, S.; Slawin, A. M. Z.; Falivene, L.; Cavallo, L.; Nolan, S. P. *Organometallics* **2013**, *32*, 3249.
(40) Jacobsen, H.; Correa, A.; Costabile, C.; Cavallo, L. *J. Organomet. Chem.* **2006**, *691*, 4350.
(41) Cordero, B.; Gomez, V.; Platero-Prats, A. E.; Reves, M.; Echeverria, J.; Cremades, E.; Barragan, F.; Alvarez, S. *Dalton Trans.* **2008**, 2832.
(42) Bondi, A. *J. Phys. Chem.* **1964**, *68*, 441.
(43) Fulmer, G. R.; Miller, A. J. M.; Sherden, N. H.; Gottlieb, H. E.; Nudelman, A.; Stoltz, B. M.; Bercaw, J. E.; Goldberg, K. I. *Organometallics* **2010**, *29*, 2176.
(44) *CrystalClear-SM Expert v2.0 and v2.1*; Rigaku Americas: The Woodlands, TX, USA, and Rigaku Corporation, Tokyo, Japan, 2010–2013.
(45) Beurskens, P. T.; Beurskens, G.; de Gelder, R.; Garcia-Granda, S.; Gould, R. O.; Israel, R.; Smits, J. M. M. *DIRDIF-99*; Crystallography Laboratory, University of Nijmegen, Nijmegen, The Netherlands, 1999.
(46) Sheldrick, G. M. *Acta Crystallogr., Sect. A* **2008**, *64*, 112.
(47) Altomare, A.; Burla, M. C.; Camalli, M.; Cascarano, G. L.; Giacovazzo, C.; Guagliardi, A.; Moliterni, A. G. G.; Polidori, G.; Spagna, R. *J. Appl. Crystallogr.* **1999**, *32*, 115.
(48) Burla, M. C.; Caliandro, R.; Camalli, M.; Carrozzini, B.; Cascarano, G. L.; De Caro, L.; Giacovazzo, C.; Polidori, G.; Spagna, R. *J. Appl. Crystallogr.* **2005**, *38*, 381.
(49) Burla, M. C.; Caliandro, R.; Camalli, M.; Carrozzini, B.; Cascarano, G. L.; Giacovazzo, C.; Mallamo, M.; Mazzone, A.; Polidori, G.; Spagna, R. *J. Appl. Crystallogr.* **2012**, *45*, 357.
(50) *CrystalStructure v4.1*; Rigaku Americas, The Woodlands, TX, USA, and Rigaku Corporation, Tokyo, Japan, 2013.